Tumor spheroids as a 3D-model for EV-mediated intratumoral RNA transfer measured by a CRISPR-Cas9 based stoplight reporter system and novel findings in the 2D model.

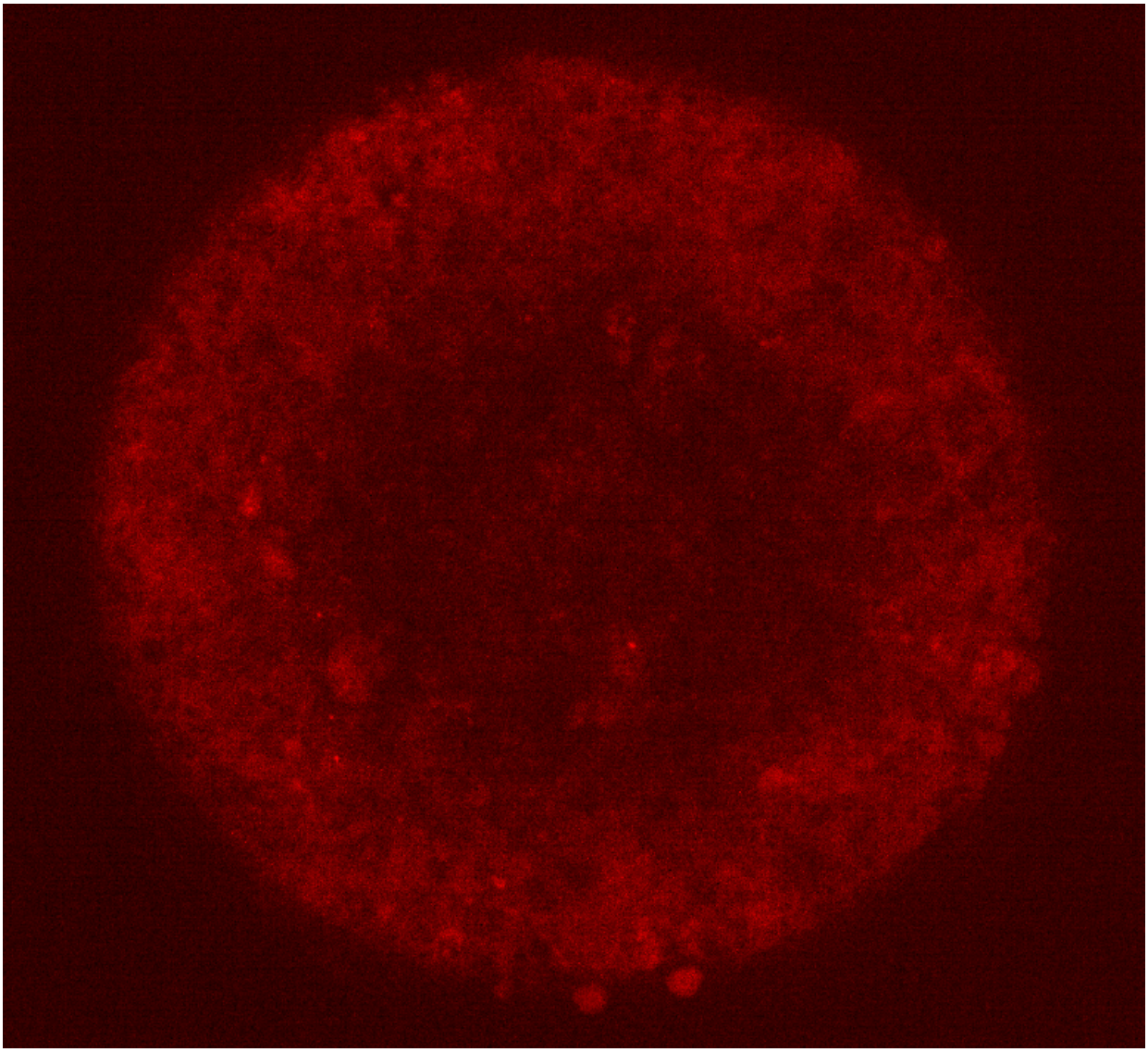

Tumor spheroid consisting of HEK293T stoplight reporter cells.

Major Research Project
Sjoerd Boonstra BSc
6749232

First examiner: dr. Olivier de Jong
Second examiner: dr. Pieter Vader

Abstract

To cope with the rising numbers of cancer diagnoses, it is necessary to develop new kinds of treatments. The tumor microenvironment (TME) could prove to be an important target for these new therapies. EV-mediated RNA transfer in the TME from high metastatic cells to low metastatic cells has proven to induce the latter to copy the behavior of the former. In this paper a CRISPR-Cas9 based stoplight reporter assay was used for measuring EV-mediated RNA transfer in a 3D model called tumor spheroids. Protocols for producing spheroids were optimized, however 3D-imaging showed these structures to be cup-shaped instead of spherical, likely limiting their use as a tumor model. Furthermore, new sgRNA expressing donor lines were created and tested using multiple stoplight reporter lines. Interestingly it was found that some donor-reporter interactions using the same cell type did not result in RNA transfer. This indicates a missing ligand-receptor interaction for uptake of EVs, which could prove to be a new therapeutic target.

Layman's summary

In the near future there will be an increase in people suffering from cancer. To cope with this, it is necessary to develop new treatments and learn more about cancer. One area of interest are the cells surrounding the tumor: the tumor microenvironment (TME). Cancer cells can change the behavior of these cells to benefit the tumor and therefore complicate cancer treatment. One factor that can induce these changes is genetic material called RNA encapsuled in so-called extracellular vesicles (EVs) released by cancer cells. Before it is possible to investigate if an inhibition of this process can be used as a treatment, it is necessary to measure the levels at which this transport takes place. To recreate the structure of a tumor, clumps of cells called tumor spheroids can be used. In this paper this system is combined with a "lock and key" system wherein the lock is a DNA fragment which induces red fluorescence in cells. The key is an RNA which is produced by cells and released in EVs. If an EV with a key inside reaches a cell with a lock, the lock can open which results in a green fluorescent cell. The amount of green fluorescent cells is now an indicator for the frequency at which this transport takes place.
It was found that the protocols used for growing tumor spheroids resulted in flat cup-shaped structures lacking the properties for a good representation of actual tumors. Also, new "key-producing" cell lines were created and tested on different "lock" cell lines. It was found that there is a cell type specificity for EV-mediated RNA transport, or in other words not all keys fit on all locks. This has not been seen before and more research on this could teach us more about this type of transport and might even lead to new therapeutic options.

Contents

Introduction

The tumor microenvironment

In 2020 worldwide 18 million patients were diagnosed with cancer, a number which will increase with 55% by 2040 (1). This drastic increase asks for new therapies and research on previously underexposed topics in cancer biology. One area of gaining interest is the tumor microenvironment (TME). The TME is a pathological environment surrounding a tumor which is in constant communication with the cancer cells. It comprises all non-cancerous components in the tumor such as fibroblasts, epithelial cells, and immune cells (figure 1). Other important factors in the TME are non-cellular contents such as the extracellular matrix (ECM), chemo-, and cytokines, growth factors and extracellular vesicles (EVs) (2,3).

The TME is sculpted by cancer cells to create a hospitable environment for the tumor by using intercellular communication mechanisms which change, among other things, cellular growth, division, and differentiation (4). This intercellular communication is largely mediated by extracellular signal molecules such as hormones and growth factors, but another important mechanism is extracellular vesicle mediated communication (5). EVs secreted by tumors have been shown to influence the TME resulting in improved tumor growth, invasion, and metastasis (3).

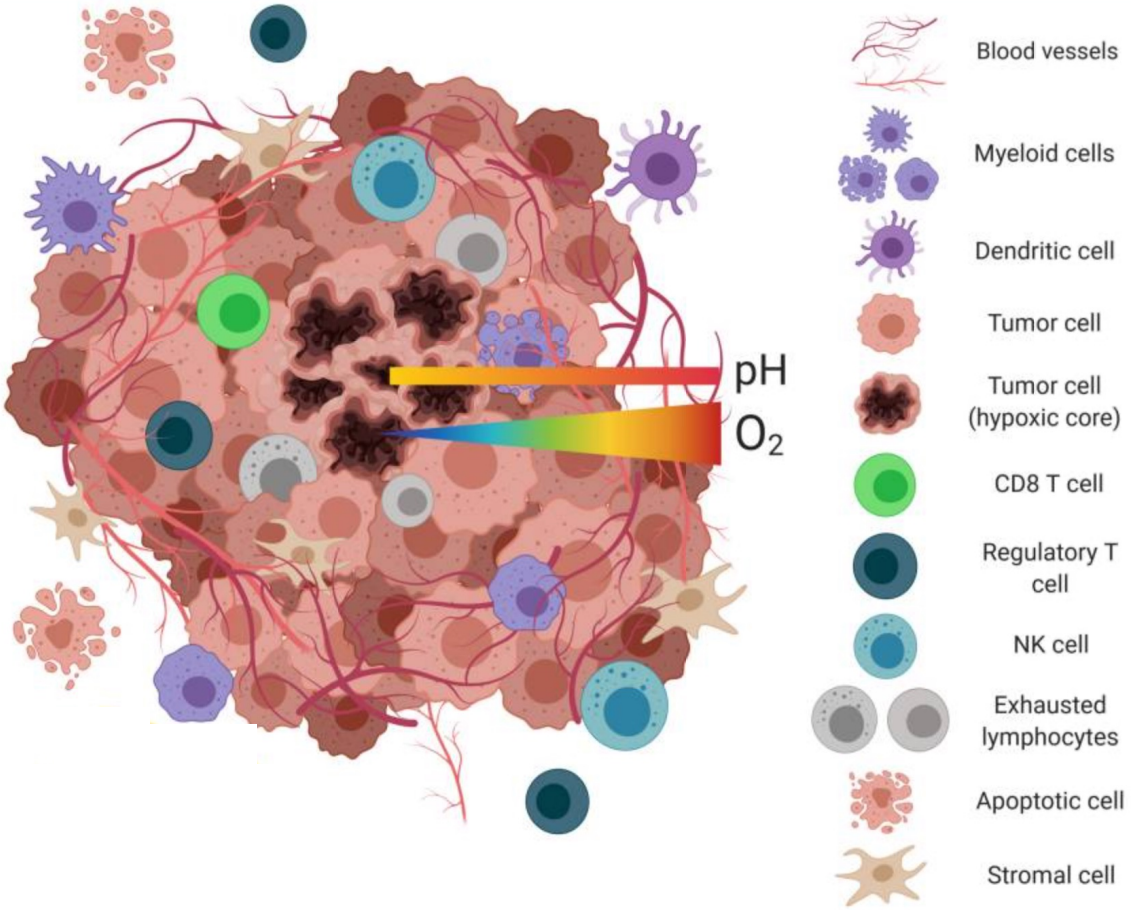

Figure 1: Different components of the tumor microenvironment. Adapted from (6)

Extracellular vesicles

Extracellular vesicles (EVs) are lipid bilayer-enclosed extracellular structures which can be produced and released by cells. EV's are divided in two different populations based on their mode of release and size. Microvesicles (MVs) are released by outward budding of the cell membrane and range from 50 to 10.000 nm. Exosomes are released in the intercellular space by fusion of the outer layers of multivesicular bodies (MVBs) with the cell membrane. MVBs in their case are formed via the inward budding of the endosomal membrane. Exosomes have a size of 30 to 150 nm (7). In this paper we investigate both microvesicles and exosomes under the overarching term of EVs. EVs are used for transportation of biological components between different cells, they can contain molecules such as proteins, sugars, and lipids, but also molecules involved in genetic information such as different types of RNA's (7).

EV-mediated RNA transfer in tumor progression

As mentioned before the bioactive cargo released by EVs can change the behavior of TME components. These changes include oncogenic recruitment, multidrug resistance, metastatic niche conditioning, tumor cell invasion, immune evasion, and stromal cell modification (figure 2) (5). This paper focuses primarily on the effect of EV-mediated RNA transport within the TME. mRNA's secreted by EVs from high metastatic cancer lines such as MDA-MB-231 have been shown to enhance migration of less metastatic cancer lines such as T47D, resulting in an increase in metastasis of T47D cells (8). This sparks the question if it is possible to inhibit EV-mediated RNA transfer, and if so, does this decrease the chances of metastasis? Before these questions can be answered it is necessary to create a model for measuring EV-mediated RNA transfer in the TME.

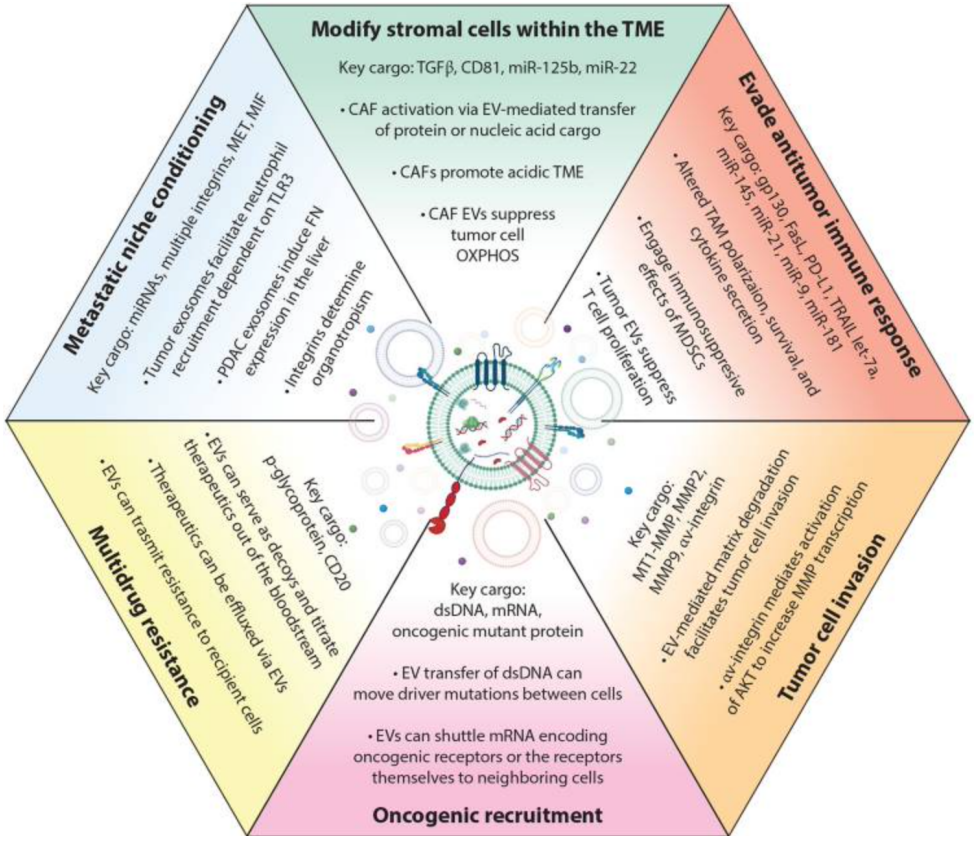

Figure 2: Effects of bioactive cargo transported by EVs within the tumor microenvironment. Adapted from: (5)

Measuring EV-mediated RNA transfer

In order to study EV-mediated RNA transfer it is necessary to measure the frequency at which this transport takes place. The CRISPR operated stoplight system for functional intercellular RNA exchange (CROSS-FIRE) was developed by de Jong et al., for this reason (9).

The clustered regularly interspaced short palindromic repeats (CRISPR)-Cas9 gene editing tool is an efficient and easy to use method with many applications both in research and recently also in therapeutics (10). It uses a sgRNA, which can bind to a complementary strand of genomic DNA, and a Cas9 endonuclease. This complex can induce a double-stranded break in the genomic DNA, leading to non-homologous end joining (NHEJ). NHEJ is an error-prone DNA repair pathway which can result in frame-shift mutations such as insertions and deletions, making CRISPR-Cas9 an excellent tool for inducing these mutations (11).

The CROSS-FIRE assay uses a constitutively expressed mCherry gene (resulting in red fluorescence) followed by a F2A self-cleavable domain and a linker. This linker contains a CRISPR-Cas9 target and a termination codon (figure 3). Under normal conditions this solely results in an expression of mCherry. The linker is however followed by two eGFP open reading frames (ORFs) which are respectively one and two nucleotides out of frame of the mCherry ORF. When a sgRNA, targeted for the Cas9 target in the linker, and a Cas9 protein are present, the resulting double-stranded break in the linker region may result in a frameshift mutation which brings the termination codon out of frame and bringing one of the eGFP genes into frame. Transcription can now take place on the eGFP gene, leading to green fluorescent cells. It is important to note that the mCherry gene remains active (9).

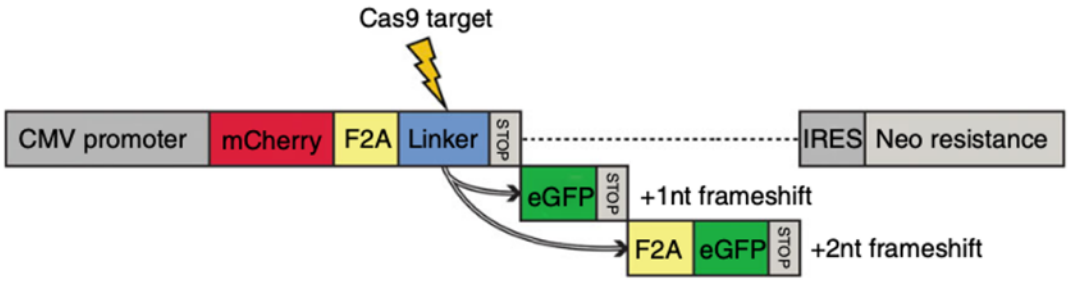

Figure 3: Schematical representation of the DNA fragment used in the CROSS-FIRE assay. Adapted from (9)

This system can be used for measuring EV-mediated RNA transfer by culturing together one cell line containing the described fluorescence reporter and stably expressing Cas9 (reporter cells) together with a cell line expressing the sgRNA (donor cells) in a co-culture assay (figure 4). The donor cells have been shown to secrete sgRNA in EVs which after uptake by reporter cells will activate the CROSS-FIRE system and induce eGFP expression. The eGFP expression can be measured by fluorescence microscopy (figure 5) as well as flow cytometry and correlates with EV-mediated transport of sgRNA (9).

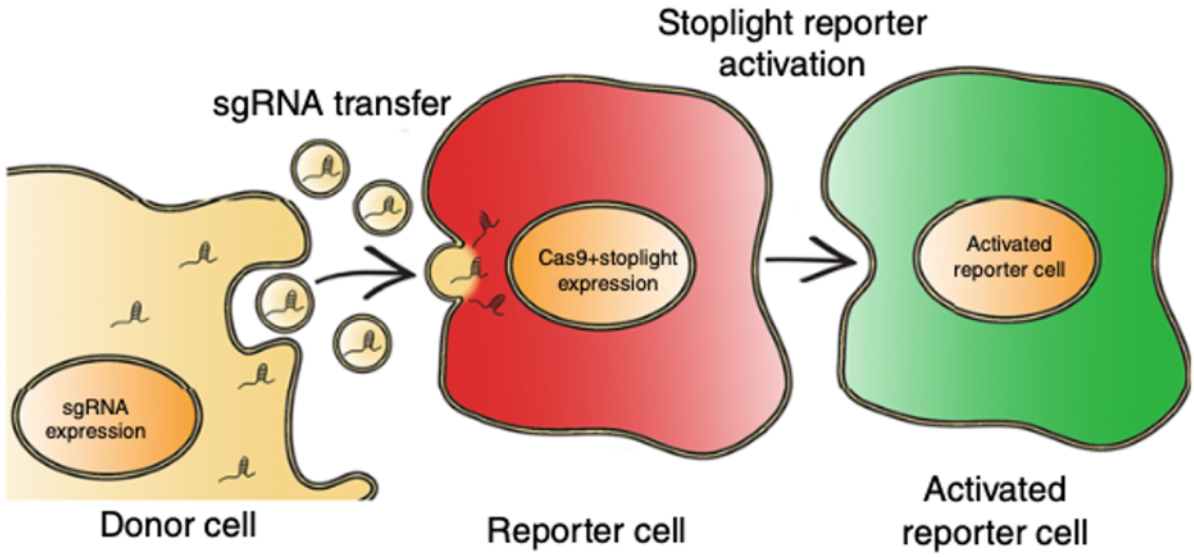

Figure 4: Schematic representation of the co-culture assay. Adapted from (9).

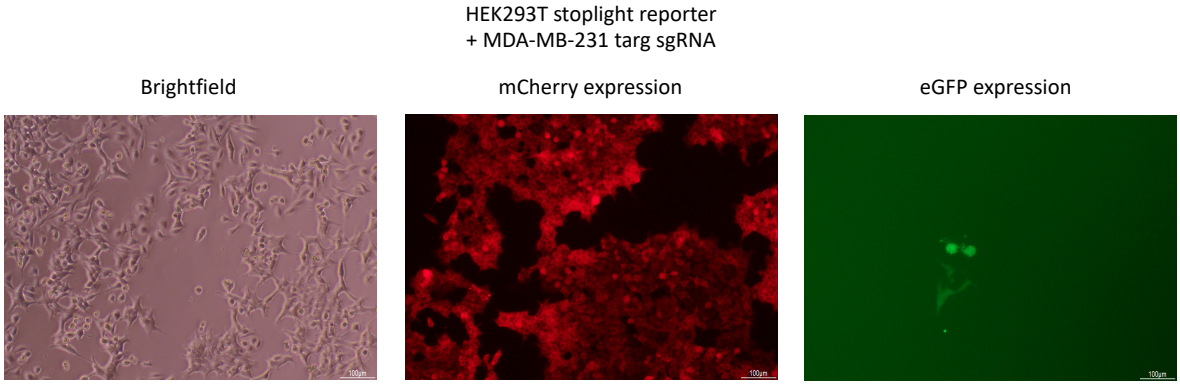

Figure 5: Fluorescence images of a co-culture assay with HEK293T stoplight reporter and MDA-MB-231 donor cells. Cultured for 5 days at a starting ratio of reporter : donor = 1:5.

Tumor spheroids

Conventional 2D cell-culture is not representative of the complex environment that tumors are. In vivo tumors are exposed to hypoxia and low nutrition as well as being influenced by intercellular communication from surrounding cells (12). A solution for this are so-called tumor spheroids, clumps of cells which mimic the behavior of tumors *in vivo*. These spheroids can produce an ECM-like structure which has been indicated to change the behavior of cells. The 3D structure also makes cells less sensitive to drug treatment due to better cell morphology and differences in surface receptors (13). Heterotypic spheroids consisting of different cell types have been shown to be good models for studying the TME (14).

There are many different protocols for spheroid formation in a broad range of complexity. One thing that many protocols have in common is that they promote cell-cell adhesion and prevent cell adhesion to cell culture plastics (15).
The hanging drop method is a cheap method for spheroid production since it uses only basic plastics commonly used in cell culture. Cells are suspended in low volumes (± 20 µL) of culture medium. This suspension can be pipetted into e.g., a wells plate with a lid. The plate is then reversed upside down causing the cell suspension to form hanging drops by surface tension. The cells are pulled down away from the plastic and towards each other by gravitational force and grow out to form spheroids after 3 days (15,16). Whilst cheap the hanging drop method is time-consuming, unsuitable for high-throughput screening and the small volumes of culture medium prevents long-term culture (17).
Suspension culture is an umbrella term for techniques using a constant motion of culture medium to prevent suspended cells from adhering to the surface of the tube or plate. The spinner culture technique uses a stirrer inside a bioreactor container to maintain this motion whilst with the "rotating wall vessel" technique the flask itself is spun. With both techniques single cells and clumps of cells can grow out to form spheroids. Suspension culture is also relatively cheap and easy to use, it is however severely limited due to the variability in the size and morphology of the created spheroids (15,16).
The liquid overlay technique (LOT) uses non-adherent materials such as agarose or hyaluronic acid to prevent cell attachment to culture plates. By centrifuging cells to the bottom of these plates, cell-cell adherence is promoted, and spheroids are formed after a few days. Manually coating these plates is very time consuming but commercial plates are available. The method is somewhat limited by the fact that not all cell types form spheroids under these conditions (15,18). One way to improve this is using hydrogels such as Matrigel or Geltrex. Hydrogels are cross-linked polymers that have biophysical and cell-adhesive properties, resulting in an ECM-like network. This network provides a scaffold for cells to adhere to and thereby improves spheroid formation (19).

The goal of this study is to develop protocols measuring EV-mediated RNA transport in a 3D tumor spheroid model using LOT and the CROSS-FIRE reporter system. Furthermore, new sgRNA donor lines were created and their ability to transfer sgRNA by EV-mediated transport was compared to other cell types in a 2D co-culture assay.

Methods

Cell culture

HEK293T, MDA-MB-231, and MCF-7 cell lines were cultured in Dulbecco's Modified Eagle Medium (DMEM) + 10% FBS + 1% antibiotics. T47D cell lines were cultured in Dulbecco's Modified Eagle Medium F12 + 10% FBS + 1% antibiotics.
Cell lines stably expressing LentiGuide Puro Tre1 (non-stoplight targeting sgRNA) or LentiGuide Puro Gal4 U6 (stoplight targeting sgRNA) were cultured with 2 µg/mL Puromycin. Cell lines stably expressing phage2-CMV-hcBFP-IRES-NeoWPRE were cultured with 500 µg/mL G418. Cells were incubated at 37°C at 5% CO2 and passaged twice per week.

2D Co-culture assay

On day 0 reporter and donor cells were seeded in a 24-wells plate with a ratio and cell count depending on their relative growth speed (table 1). Cells were cultured in DMEM + 10% FBS + 1% antibiotics without additional selection antibiotics. On day 2 half the wells with stoplight reporter only were transfected with 500 ng LentiGuide Puro Gal4 U6 (stoplight targeting sgRNA) with a Plasmid:PEI ratio of 1:3 as a positive control. Concentrations of PEI and the plasmid were added to separate tubes containing OptiMEM and incubated for 5 min at RT, after which both tubes were mixed and incubated for 15 min at RT. Final concentration was 500 ng plasmid in 100 µL OptiMEM. 100 µL of mix was added per well. At day 5 cells were imaged with fluorescence microscopy and prepared for flow cytometry. Medium was removed and cells were washed with PBS. Trypsin was added and the plate was incubated for 5 min at 37°C. Medium was added and cells were resuspended and transferred to Eppendorf tubes. Cells were spun down at 300 x g for 5 min. Supernatant was removed and cells were resuspended in PBS. PBS was removed and cells were either resuspended in 100 µL PBS + 1% FBS or fixated in 1% PFA after which they were transferred to a 96 round-bottom well plate and stored at 4°C.

Table 1: Ratios of reporter to donor for multiple cell lines on d0. Total number of cells between 24.000 and 30.000.

Stoplight reporter line	Donor line	Ratio
HEK293T	MDA-MB-231	1:5
HEK293T	MCF-7	1:5
HEK293T	T47D	1:8
MCF-7	MDA-MB-231	1:5
MCF-7	MCF-7	1:1
MCF-7	T47D	1:3
MDA-MB-231	MCF-7	1:1
MDA-MB-231	T47D	1:1
T47D	MCF-7	1:1
T47D	T47D	1:1

Spheroid production

On day 0 cells were seeded in Corning® Ultra-Low Attachment Surface, round bottom, clear, 96 well plate. Number of cells was variable but was usually set at 10.000 cells per well. The plate was centrifuged at 300 x g for 5 min and incubated for 5 days at 37°C at 5% CO_2. Optionally Matrigel or Geltrex was added to the medium either immediately after centrifuging or after 24h.

Generating stable cell lines

Virus production

At day 0 HEK293T WT cells were passaged to a T75 at 30-50% confluency. On day 1, at the end of the day, cells were transfected with 5 µg PSPAX2, 5 µg pVSV-G, and 10 µg lentiviral plasmid with the gene of interest. On the morning of day 2 the transfection mix was removed by refreshing the medium. Medium containing the lentiviral supernatant was harvested on the morning of day 4. Supernatant was centrifuged for 5 min at 500 x g and isolated and filtered through a 0.45 µm filter. Aliquots of the lentiviral supernatant were stored at -80°C.

Transducing cells with lentiviral supernatant

Cells were passaged to a T25 at a confluency of 50-60% on day 0. At the end of day 1 2 mL of lentiviral supernatant was added. On the morning of day 2 lentiviral supernatant was removed by refreshing the medium. Selection antibiotics were added on day 3, for both puromycin and G418 a concentration of 2 µg/mL was used. Cells were cultured for 2 weeks before being scaled down to ML-1 and cultured in lower concentrations of selection antibiotics (see: cell culture).

Yokogawa analysis of 3D cultures

Microscope for 3D imaging and BFP imaging used is the Yokogawa CV7000S Cellvoyager. Descending distance was set at -125.0 um, shifting distance at 50.0 um, ascending distance at 200.0 um, and slicing interval at 10.0 um. Fluorescence images were taken at 10x magnification, brightfield images at 20x.
All pictures from one well and one channel were transformed into stacks with Fiji version 2.9.0./1.53t.

3D reconstruction of spheroids

3D images were made using the 3D viewer plugin of Fiji version 2.9.0./1.53. Previously made stacks of 3D imaging were adjusted for brightness and uploaded in the 3D viewer. The 3D viewer was set on surface and the threshold was set to 30. The threshold and/or brightness was changed if no clear 3D rendering was formed.

Flow cytometry analysis

Medium was aspirated and cells were washed in PBS. 200 µL Trypsin EDTA was added and incubated for 5 min at 37°C. Cells were resuspended in medium and transferred to Eppendorf tubes. Cells were centrifuged at 300 x g for 5 min after which the supernatant was removed. The cells were washed in PBS followed by centrifuging at 300 x g for 5 min. Supernatant was removed and cells were resuspended in 100 µL PBS + 1% FBS or fixated in 1% PFA and transferred to a 96 well plate.
Flow cytometry was performed using different flow cytometry systems: FACS Fortessa, FACS Canto and CytoFLEX LX. All data was analyzed using FlowLogic software. Gating strategy was determined by negative and positive controls (see figure 13).

Spheroid disruption

6 spheroids were transferred to one Eppendorf tube with a p1000 with a part of the pipet tip cut off. Spheroids were centrifuged for 5 min at 300 x g. Medium was aspirated and spheroids were washed in PBS. 200 µL 1x trypLE was added and incubated for 20 min at 37°C (in-between vortexing might improve spheroid disruption). Tubes were vortexed and culture medium was added. After washing with PBS samples were put through a 70 µm cell strainer to prevent clogging of the FACS. Cells were centrifuged at 300 x g for 5 min after which the supernatant was removed, and cells were either resuspended in 100 µL PBS + 1% FBS or fixated and transferred to a 96 well plate (figure 6).

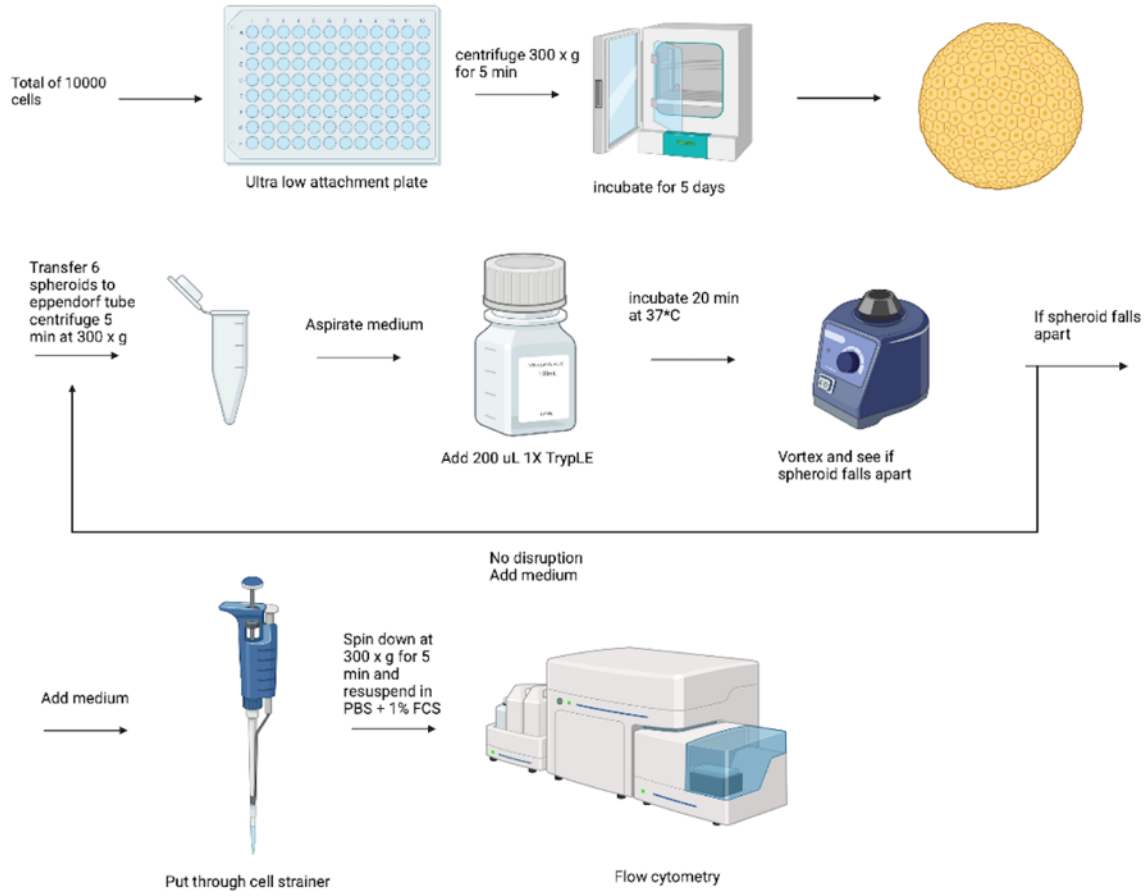

Figure 6: Protocol for disruption of spheroids to single cells for flow cytometry analysis.

Cloning of nuclear localizing BFP plasmid

The puromycin resistance gene was cut from plasmid FUW-EF1a-H2B-mTAG_BFP-IRES-PuroR-WPRE and replaced with a blasticidin resistance gene cut from plasmid pHAGE2-CMV-MCS-IRES-Blast-WPRE. For maps of plasmids see supplementary figures 1 to 3.
Both plasmids were restricted in a mix of 2 µg plasmid, 2 µL NEBuffer CutSmart, 1 µL NdeI enzyme, 1 µL ClaI enzyme, and ddH20 was added to a total volume of 20 µL. The mix was incubated for 30 min at 37°C. 2% TAE agarose gel with 1:25000 Midori Green was prepared and loading buffer was added to the restricted plasmids followed by loading of the mix on the gel. Sample was run for 1 hour at 150 volts. Correct fragments were cut out of the gel. A ligation mix was made by adding 2 µL vector backbone, 6 µL insert, 2 µL 10x T4 ligase buffer, 10 µL ddH2O and 1 µL T4 ligase. As a control a mix without insert was made. 2.5 µL of ligation mix was added to 25 µL of Stbl3 E. coli in Zymo buffer, which was incubated for 10 min on ice. 200 µL of LB broth was added and the mix was incubated for 45 min at 37°C. Both mixes (+insert and -insert) were plated out on LB-Agar-Ampicillin plates and incubated overnight at 37°C. 8 colonies on the +insert plate were picked from the plate and grown in 5 mL LB medium + ampicillin and incubated overnight at 37°C at 200 – 250 rpm. Miniprep was performed on all samples using the GeneJET Plasmid Miniprep Kit followed by sequencing. The sample containing the correct plasmid was further amplified in 100 mL LB medium + ampicillin after which a midiprep was performed using the PureLink™ HiPure Plasmid Midiprep Kit according to the manufacturer's protocol.

Results

Optimization of spheroid formation

Three different cell types were tested for their ability to form spheroids in LOT ultra-low attachment plates. The Human Embryonic Kidney (HEK)293T is a highly transfectable kidney derived epithelial-like cell line (20). HEK293T was picked because of its ease of use and its proven effectiveness as a stoplight reporter in the CROSS-FIRE assay (9). MDA-MB-231 was derived from the mammary gland of a patient with adenocarcinoma and is an epithelial-like cell (21). It is highly metastatic and is often used as a model for triple-negative breast cancer (22). MDA-MB-231 was used because of its effectiveness as a sgRNA producing donor cell and because it is a cancer cell line, which is relevant to this paper (9). MCF-7 is also a mammary gland derived epithelial cancer cell line. The cell line is non-metastatic and therefore often used as a model for early-stage cancer (22). MCF-7 was mainly chosen for its cancer origin.

Effect of size and cell type

When comparing the ability of different cell types to form spheroids both HEK293T and MCF-7 showed round and dense structures after 5 days of culturing whilst MDA-MB-231 showed a loose population of cells (figure 7A).
To test the effect of different cell counts on spheroid formation both high- and low numbers of cells were used. HEK293T cells showed to form round and dense structures in all conditions, getting slightly non-spherical (egg-shaped) from 20.000 cells to higher (figure 7B).

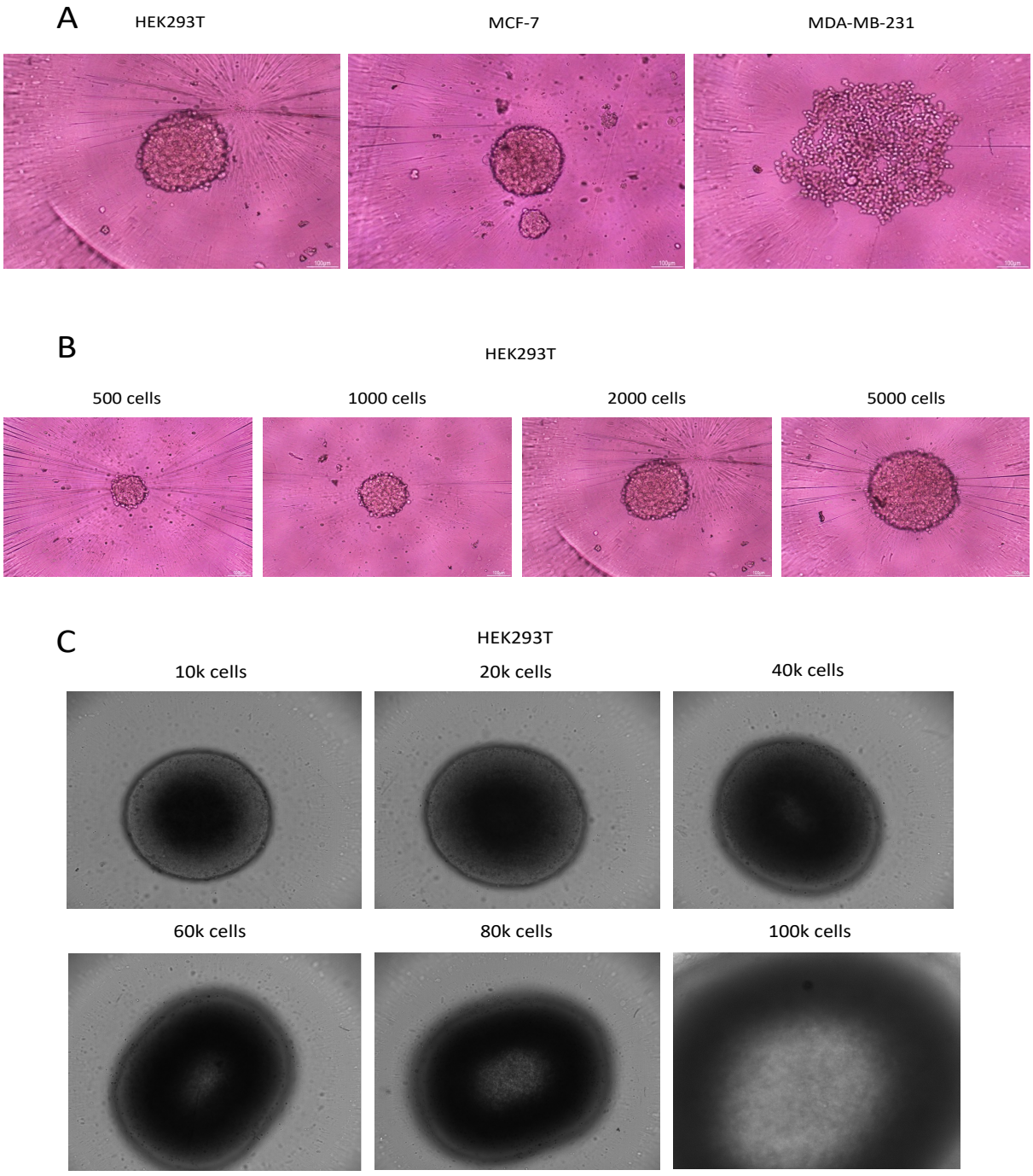

Figure 7: A: Spheroids form HEK293T, MCF-7, and MDA-MB-231 cell lines. 2000 cells were seeded on day 0. B: Spheroids from HEK293T cells in a low range. C: Spheroids from HEK293T cells in a high range. All images taken after 5 days of culturing in DMEM + 10% FBS. Numbers refer to number of cells seeded at day 0. All conditions were centrifuged at 300 x g for 5 min on day 0. Scalebars in panel A/B = 100 µm.

Effect of different types of medium on spheroid formation

To compare effects of different types of medium DMEM + 10% FBS was compared to PromoCell® 3D Tumorsphere Medium XF (Tumed), which according to the manufacturer is specialized for the isolation and 3D long-term cultivation of cancer cells (23). The medium has been used in other papers but no papers comparing this specialized medium to regular cell culture medium have been published (24). In parallel with this comparison in use of medium, the effect of centrifuging the plate after cell seeding was studied on the hypothesis that by physically bringing cells closer by centrifuging more cell-cell interactions are formed resulting in denser spheroids. On the other hand, centrifuging causes mechanical stress on cells, likely decreasing viability.

Spheroid formation in Tumed showed irregularly shaped spheroid formation for HEK293T and MCF-7 compared to the more circular structures in the DMEM condition. No difference could be seen in spheroid formation for MDA-MB-231 when comparing media.

Spheroid formation in Tumed did not change regardless whether the plate was centrifuged or not (figure 8A/B). A comparison of centrifuging with DMEM proved to be unusable for publication. 3D-renderings (see methods) were made by measuring the mCherry signal in the HEK293T stoplight reporter line, which showed that the uncentrifuged Tumed condition appears to be a flat layer of cells (figure 9A/B/C). The DMEM condition with centrifuge shows a cup-shaped structure (figure 9D/E/F). This cup-shaped form will most likely allow nutrients to reach the inner cells of the spheroid preventing a necrotic core from forming. Since this is one of the main advantages of using tumor spheroids this should be further improved.

Because of its circular and dense structures, it was decided to continue using DMEM. Although an effect of centrifuging could not be concluded the step was integrated in the protocol because literature showed it to prevent formation of multiple smaller spheroids instead of the favorable situation of one larger spheroid per well (25).

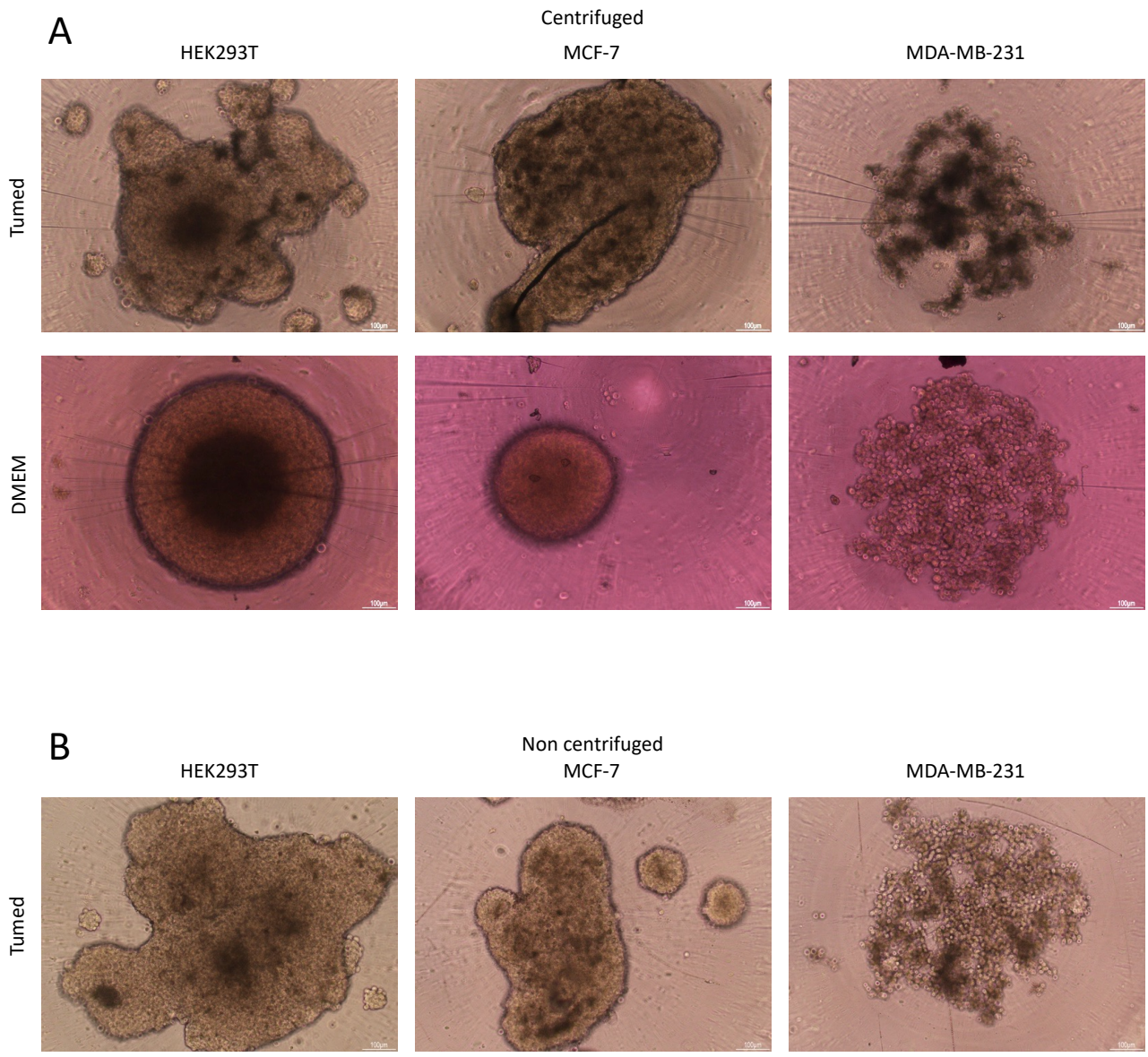

Figure 8: A: Spheroid formation of HEK293T, MCF-7, and MDA-MB-231 cell lines in DMEM compared to Tumorsphere medium. Centrifuged at 300 x g for 5 min. B: Spheroid formation of HEK293T, MCF-7, and MDA-MB-231 cell lines in Tumorsphere medium. Not centrifuged. For all conditions 1000 cells were seeded at day 0. Imaged on day 5. All scalebars are 100 µm.

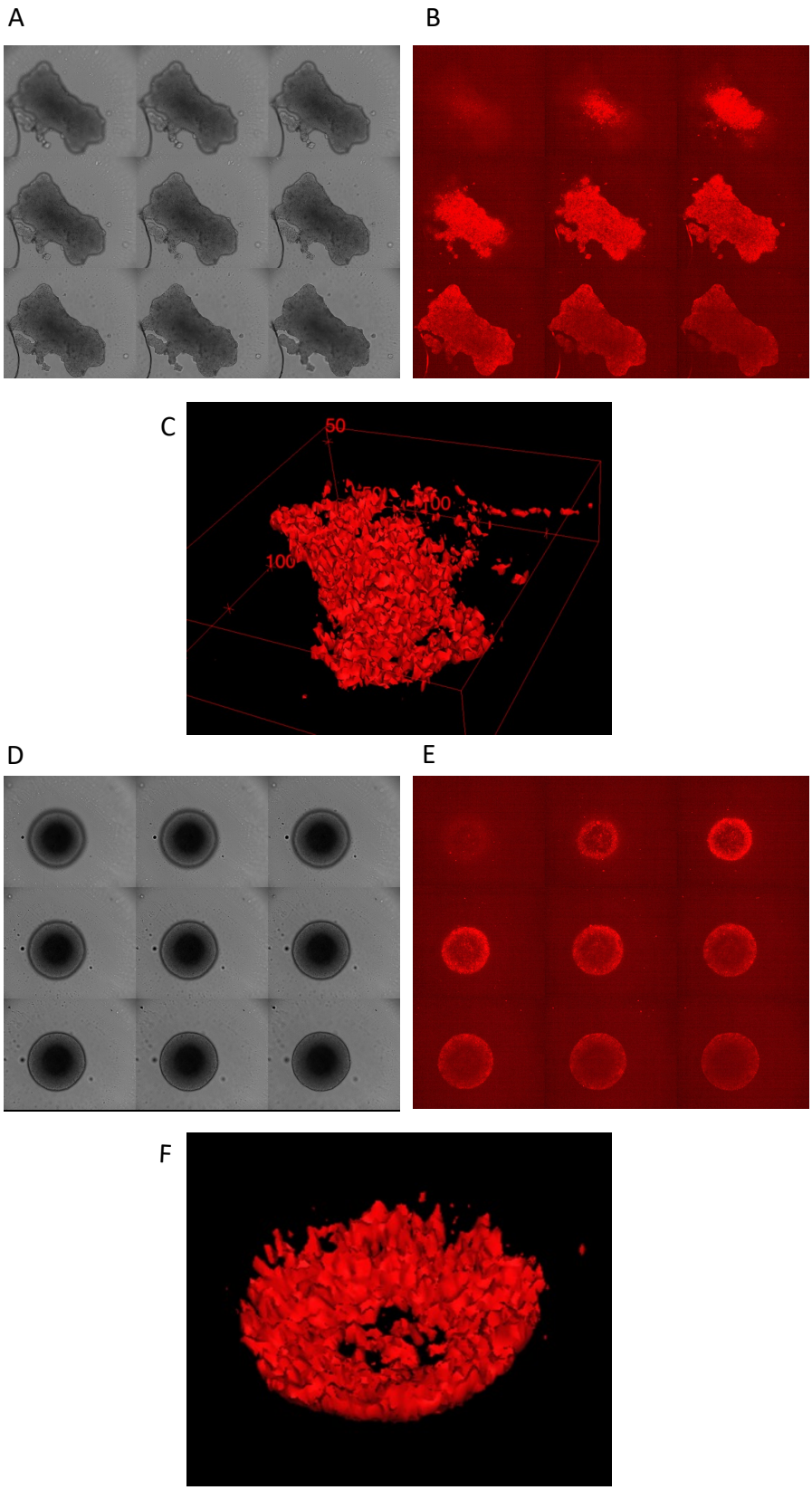

Figure 9: A/B/C: 3D imaging and reconstruction of HEK293T stoplight reporter cultured in Tumed at day 5 Uncentrifuged. D/E/F: 3D imaging and reconstruction of HEK293T stoplight reporter cultured in DMEM at day 5. Centrifuged at 300 x g for 5 min. All conditions: On day 0 10.000 cells were seeded. Distance between slices 20 µm.

Spheroid formation in low percentages of Geltrex or Matrigel

To improve spheroid formation both Geltrex and Matrigel were used in low percentages. Geltrex and Matrigel provide a scaffold for cells to adhere to and has been shown to improve formation of 3D structures (25,26). Figure 10A shows low percentages of both Geltrex and Matrigel results in adherence of the cells to the bottom of the well, creating a flat layer of cells. Adding 2% Geltrex resulted in the densest structure, however 3D rendering (figure 10B/C/D) shows a hollow spheroid. There appears to be somewhat of an improvement compared to figure 9F, but the hollowness is still suggested to prevent the formation of a necrotic core.

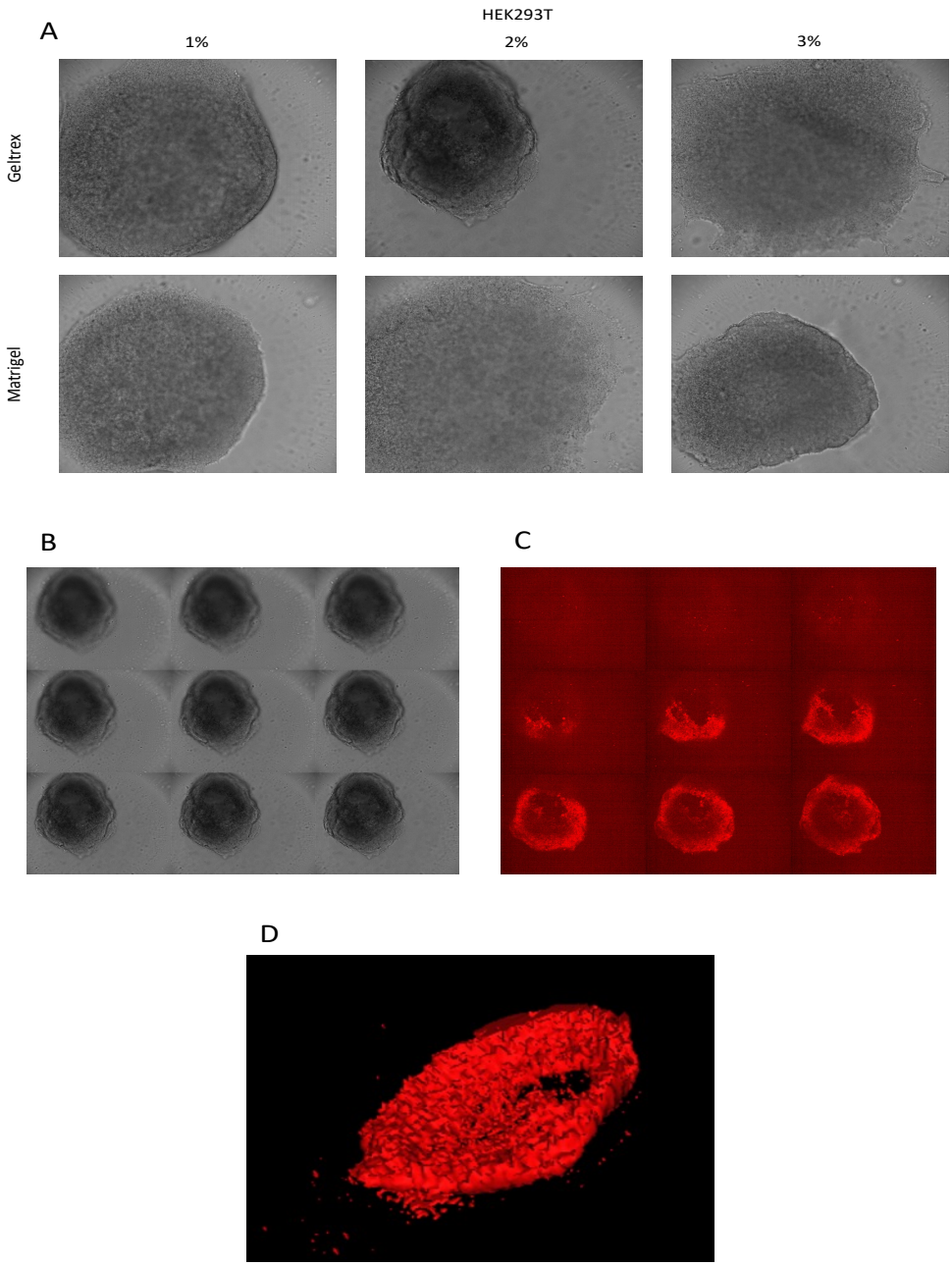

Figure 10: A: Spheroid formation of HEK293T cells under influence of different percentages of Geltrex or Matrigel added at day 0, 10.000 cells seeded and centrifuged at 300 x g for 5 min. Cultured in DMEM. Imaged on day 5. B/C/D: 3D imaging and reconstruction of HEK293T stoplight reporter cultured in DMEM + 2% Geltrex at day 5. On day 0 10.000 cells were seeded and centrifuged at 300 x g for 5 min. Tilted view. Distance between slices 20 µm.

Combinations of different cell types

In order to perform a 3D co-culture assay, it was investigated if it is possible to make heterotypic spheroids consisting of different cell types. As can been seen in figure 11A, a combination of HEK293T and MCF-7 resulted in structures where different cell types were indiscernible from each other. For HEK293T and MDA-MB-231 both populations can be clearly discerned from each other, HEK293T cells show small round structures in a “cloud” of MDA-MB-231 cells.

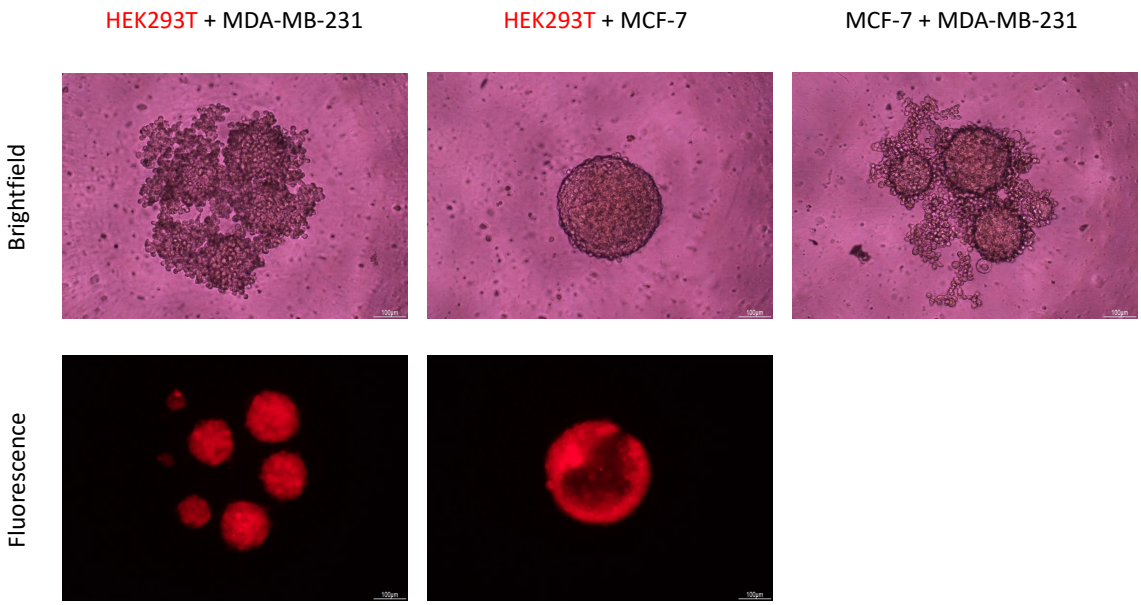

Figure 11: Spheroid formation of combinations of different cell types. 1000 cells of each cell type seeded at day 0. Centrifuged at 300 x g for 5 min. Only HEK293T shows red fluorescence. Imaged at day 3. All scalebars 100 µm.

A combination of HEK293T and MDA-MB-231 with low percentages of Geltrex (figure 12) showed a better mix of both cell types, but since the effect of Geltrex/Matrigel on EV-mediated intercellular communication remains unknown, the combination of HEK293T and MCF-7 without Geltrex was tested first.

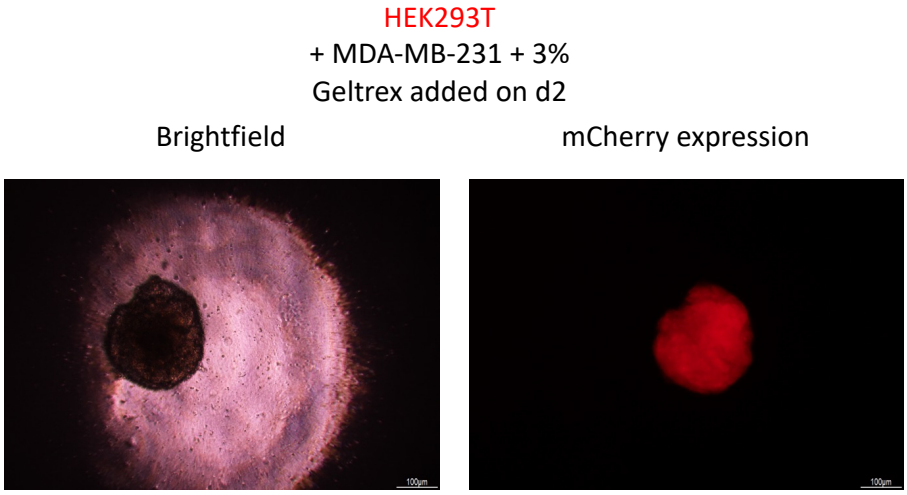

Figure 12: Combination of HEK293T and MDA-MB-231 under the influence of 3% Geltrex added on day 2. Imaged on day 5. All scalebars are 100 µm.

Flow cytometry analysis of 3D spheroid cultures

In order to measure EV-mediated RNA transfer by a 3D co-culture assay it is necessary to disrupt spheroids to single cells to measure eGFP expression by flow cytometry. First experiments showed disrupting one spheroid to single cells results in a low number of events. A combination of six spheroids in one sample showed higher numbers of events, which is necessary for more accurate results. This protocol (see methods) was further optimized and shown to successfully disrupt spheroids to single cells after which mCherry and eGFP signals could be measured (figure 13).

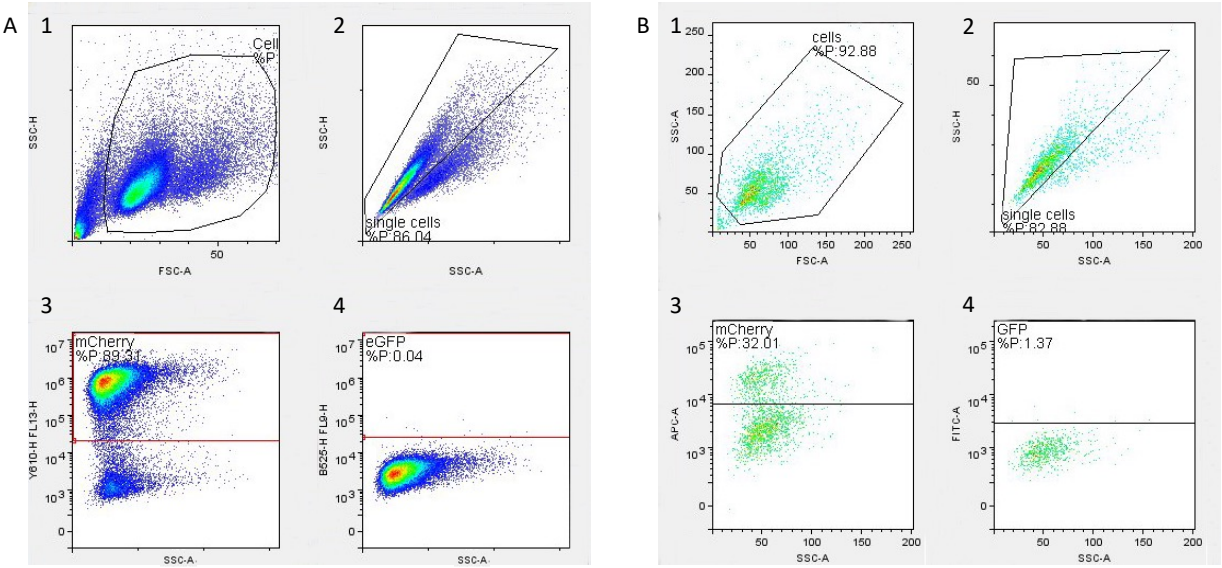

Figure 13: Flow cytometry data of spheroids consisting of a 1:5 ratio of HEK293T stoplight reporter and MCF-7 targeting sgRNA with a total of 10.000 cells on day 0. Spheroids disrupted on day 5. A: Disruption of 6 spheroid in one tube. B: Disruption of one spheroid in one tube. A/B: 1: Cell selection. 2: Single cell selection. 3: mCherry+ gating (reporter cell selection). 4: eGFP+ measurement (within mCherry+ population).

Spheroid formation using ultra-low attachment plates resulted in hollow, cup shaped spheroids most likely incapable of forming a necrotic core. It is also hypothesized that EVs behave different in a cup-shaped spheroid compared to a denser spheroid. EVs in a compact spheroid will be taken up by cells in proximity to the cell which released the EV. Spheroids with an open structure will see EV-mediated RNA transfer over longer distances. Whilst it was proven possible to disrupt spheroids to single cells for measuring EV-mediated RNA transfer, spheroids should better mimic an *in vivo* tumor before conclusions can be drawn.

Creating and testing new sgRNA expressing donor lines

Because of the inability of the MDA-MB-231 sgRNA donor cells to form spheroid-like structures in Geltrex/Matrigel-free conditions new sgRNA expressing donor lines were made by lentiviral transduction (see methods). Since MCF-7 and T47D had already shown to form spheroids without Geltrex or Matrigel (supplementary figure 4, figure 7A). For both T47D and MCF-7 stoplight targeting, and non-targeting donor lines were made which were tested in a co-culture assay (see methods) with multiple stoplight reporter lines.

MCF-7 donor lines

The MCF-7 targeting- and non-targeting donor lines were tested in combination of both HEK293T stoplight reporter as well as the MCF-7 stoplight reporter. eGFP expression was measured by flow cytometry. Reporter lines transfected with targeting sgRNA were used as a positive control but excluded from graphs. The combination of HEK293T stoplight reporter and MCF-7 targeting sgRNA resulted in a much higher and more significant change in eGFP expression compared to the existing MDA-MB-231 donor lines (figure 14A/B). Interestingly, a combination of MCF-7 targeting sgRNA and MCF-7 stoplight reporter did not result in a significant change in eGFP expression (figure 14C/D). This cell type specificity for EV-mediated RNA exchange has not been seen before and raises questions about the underlying mechanism causing this and its possible therapeutic applications. MCF-7 non-targeting donor cells showed no significant increase in eGFP expression in both stoplight reporter lines, confirming its usability as a control. eGFP expression was visually confirmed by fluorescence microscopy (figure 14A/C).

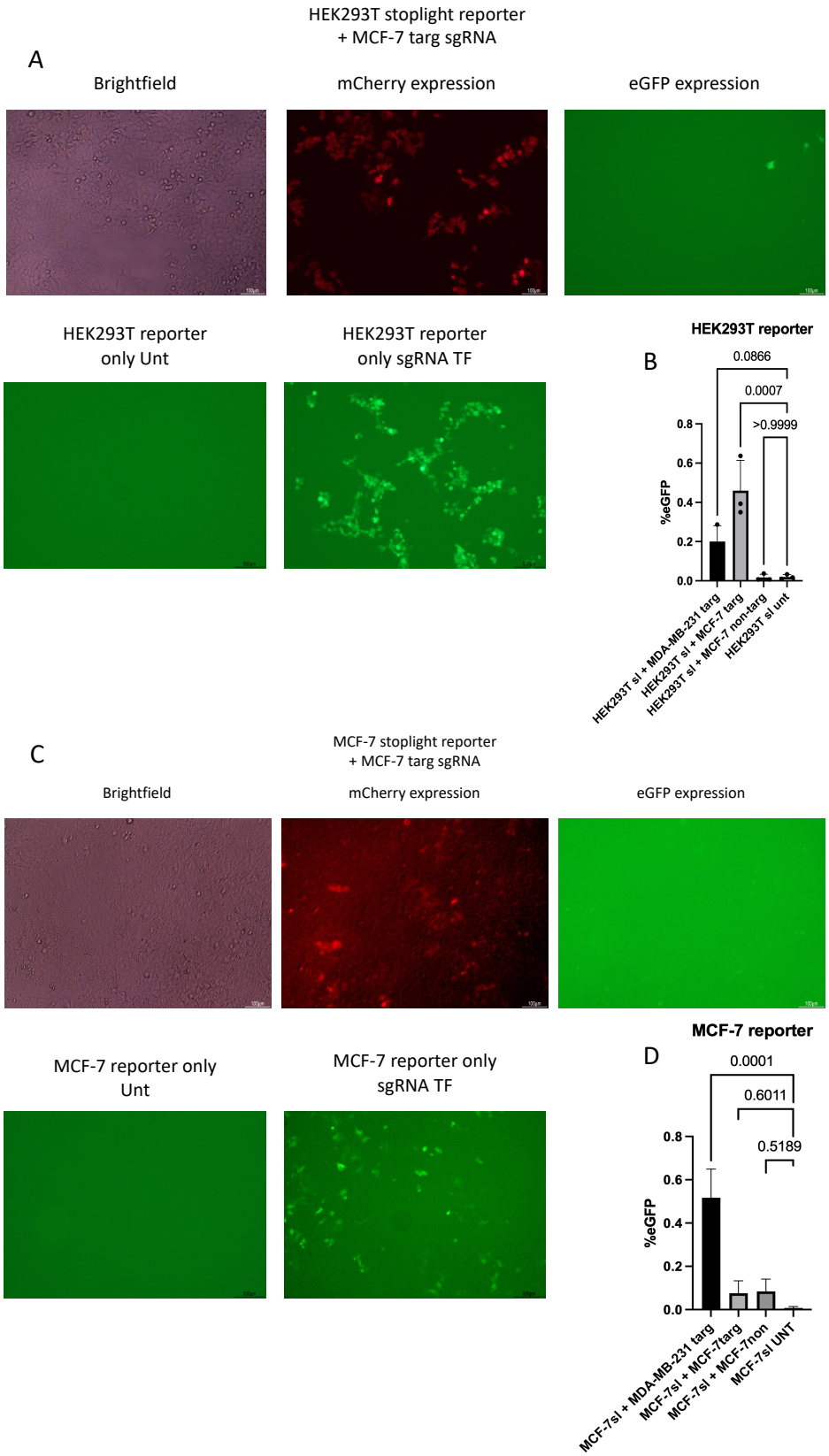

Figure 14: A: fluorescence microscopy images of the co-culture assay of HEK293T stoplight reporter and MCF-7 targ sgRNA donor line. Cultured for 5 days on a ratio of 1:5 on day 0. B: Statistical analysis of multiple donor lines with HEK293T stoplight reporter. Ordinary one-way ANOVA was performed. N=3. C: Fluorescence microscopy images of the co-culture assay of MCF-7 stoplight reporter and MCF-7 targ sgRNA donor line. Cultured for 5 days on a ratio of 1:1 on day 0. D: Statistical analysis of multiple donor lines with MCF-7 stoplight reporter. Ordinary one-way ANOVA was performed. N=3. All scalebars are 100 µm.

T47D donor lines

T47D is an epithelial, mammary-derived cancer cell line which is non-metastatic (27,28). T47D donor cells were also made using lentiviral transduction and showed no significant increase in eGFP expression in all tested stoplight reporter lines (figure 15/16). Although combinations with MDA-MB-231- and T47D stoplight reporter lines were only performed N=2 and there are some outliers in the data, it is safe to assume that T47D donor cells produce insufficient sgRNA containing EVs to induce eGFP expression in all tested stoplight reporter lines.

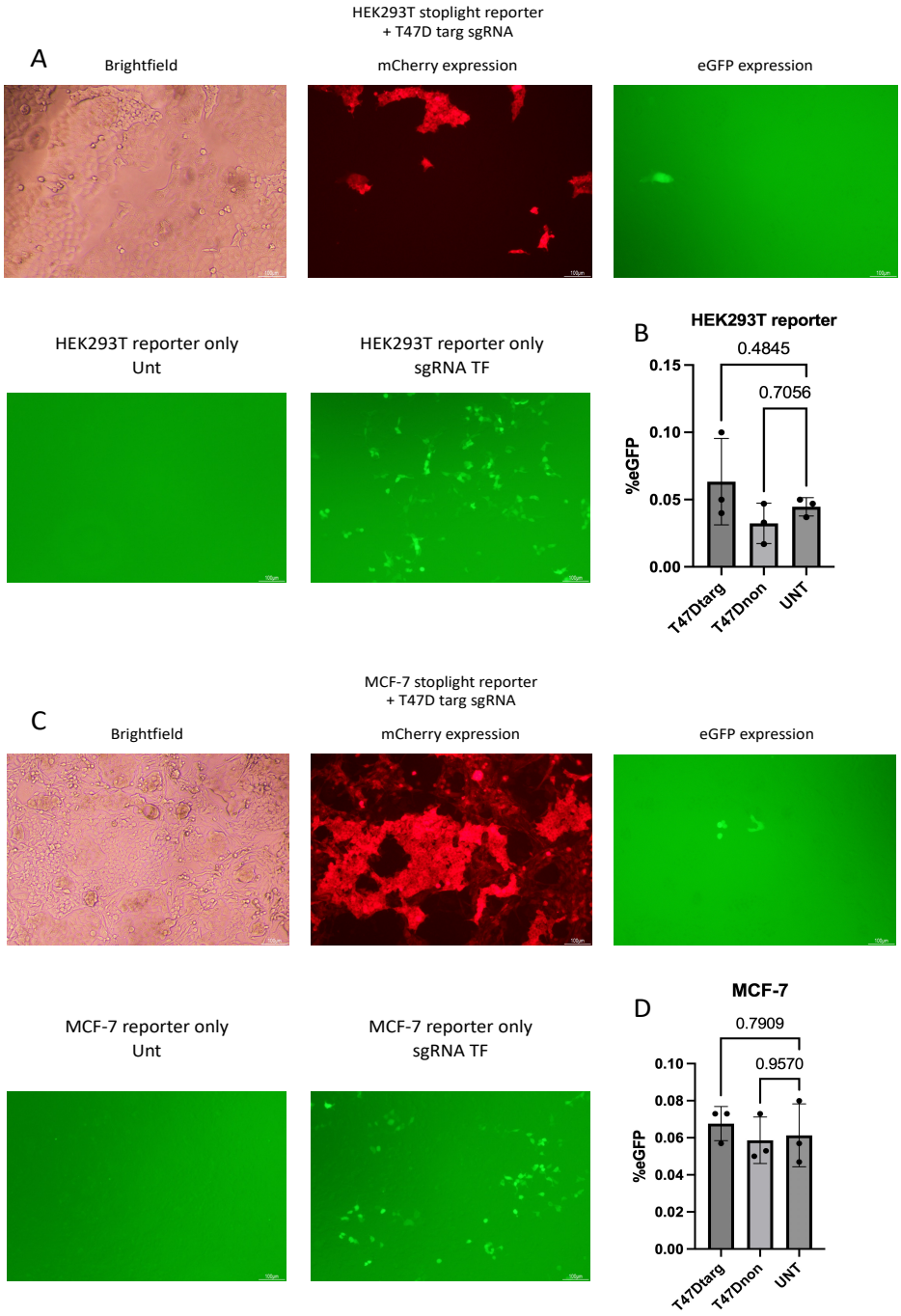

Figure 15 A: co-culture assay of HEK293T stoplight reporter and T47D targ sgRNA donor line. Cultured for 5 days. B: Statistical analysis of T47D donor lines with HEK293T stoplight reporter. Ordinary one-way ANOVA was performed. N=3 C: co-culture assay of MCF-7 stoplight reporter and T47D targ sgRNA donor line. Cultured for 5 days. D: Statistical analysis of T47D donor lines with MCF-7 stoplight reporter. Ordinary one-way ANOVA was performed. N=3. All scalebars 100 µm.

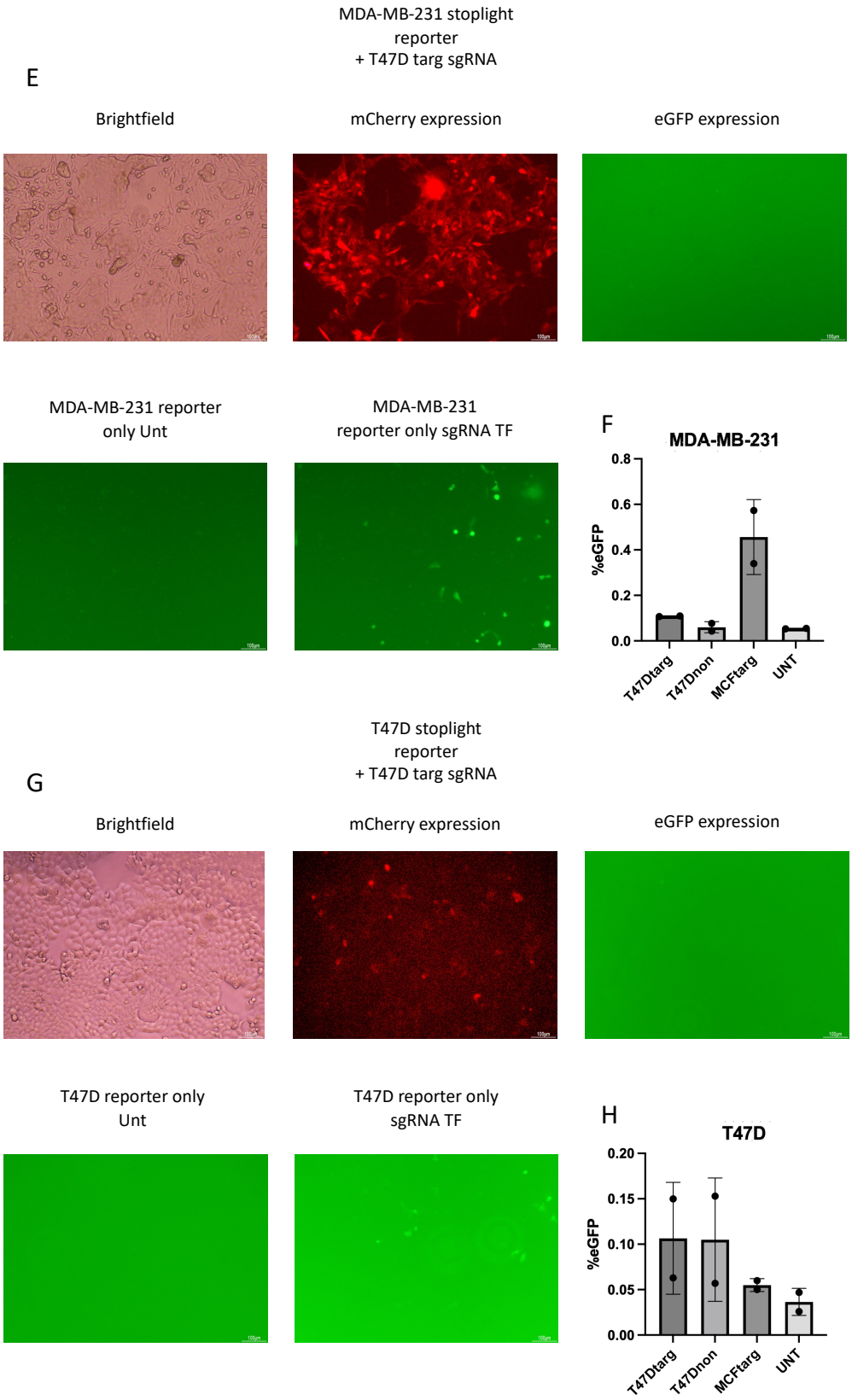

Figure 16 A: co-culture assay of MDA-MB-231 stoplight reporter and T47D targ sgRNA donor line. Cultured for 5 days. B: Statistical analysis of T47D donor lines with MDA-MB-231 stoplight reporter. Ordinary one-way ANOVA was performed. N=3 C: co-culture assay of T47D stoplight reporter and T47D targ sgRNA donor line. Cultured for 5 days. D: Statistical analysis of T47D donor lines with T47D stoplight reporter. Ordinary one-way ANOVA was performed. N=3. All scalebars are 100 µm.

Creating and testing new BFP expressing cell lines

Lastly, in order to be able to discern mCherry stoplight cells from donor cells without fluorescence, these donor lines were transduced to stably express BFP with the phage2-CMV-hcBFP-IRES-Neo-WPRE plasmid. This was preferred to staining with nuclear dyes such as DAPI and Hoechst, which have shown to induce cytotoxicity and are unlikely to penetrate to the inner cells of spheroids (29). Also, a previously made plasmid (FUW-EF1a-H2B-mTAG_BFP-IRES-PuroR-WPRE) containing a BFP gene which localizes in the nucleus was modified for use in donor cells by exchanging the puromycin resistance gene for a blasticidin resistance gene which was necessary because the plasmid for sgRNA expression already contains a puromycin resistance gene. This plasmid (FUW-EF1a-H2B-mTAG_BFP-IRES-BlastR-WPRE, supplementary figure 3) uses an mTAGBFP2 protein to bind to human histone H2B, showing blue fluorescence in the nucleus(30). Flow cytometry analysis showed BFP expression in lentivirally transduced cells ranging from 40-70% (figure 17). These percentages are sufficient for fluorescence microscopy (figure 18). For identifying BFP+ donor cells with flow cytometry it could prove beneficial to use a cell sorting system to increase these percentages.

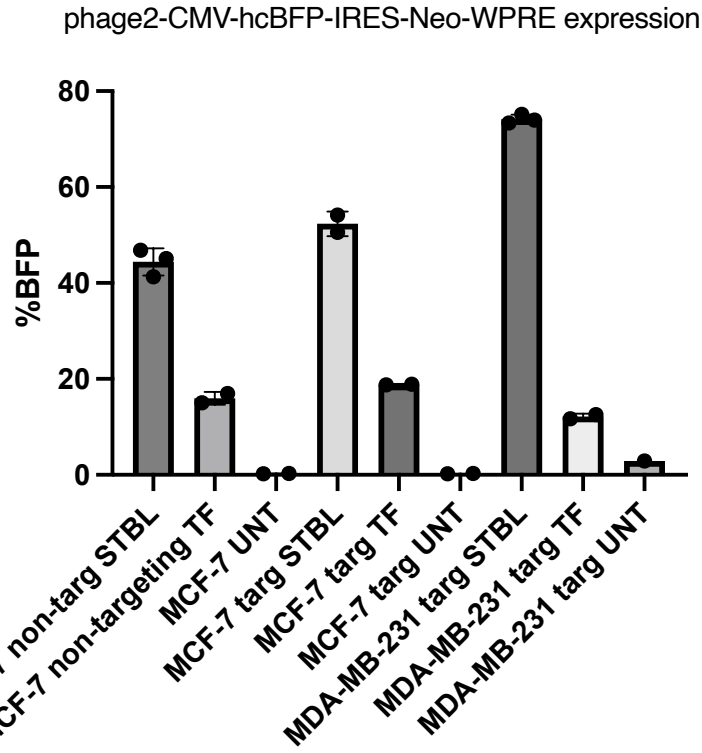

Figure 17: Percentage of BFP positive cells of different cell lines after lentiviral transduction (STBL) or after transfection (TF) with the phage2-CMV-hcBFP-IRES-Neo-WPRE plasmid.

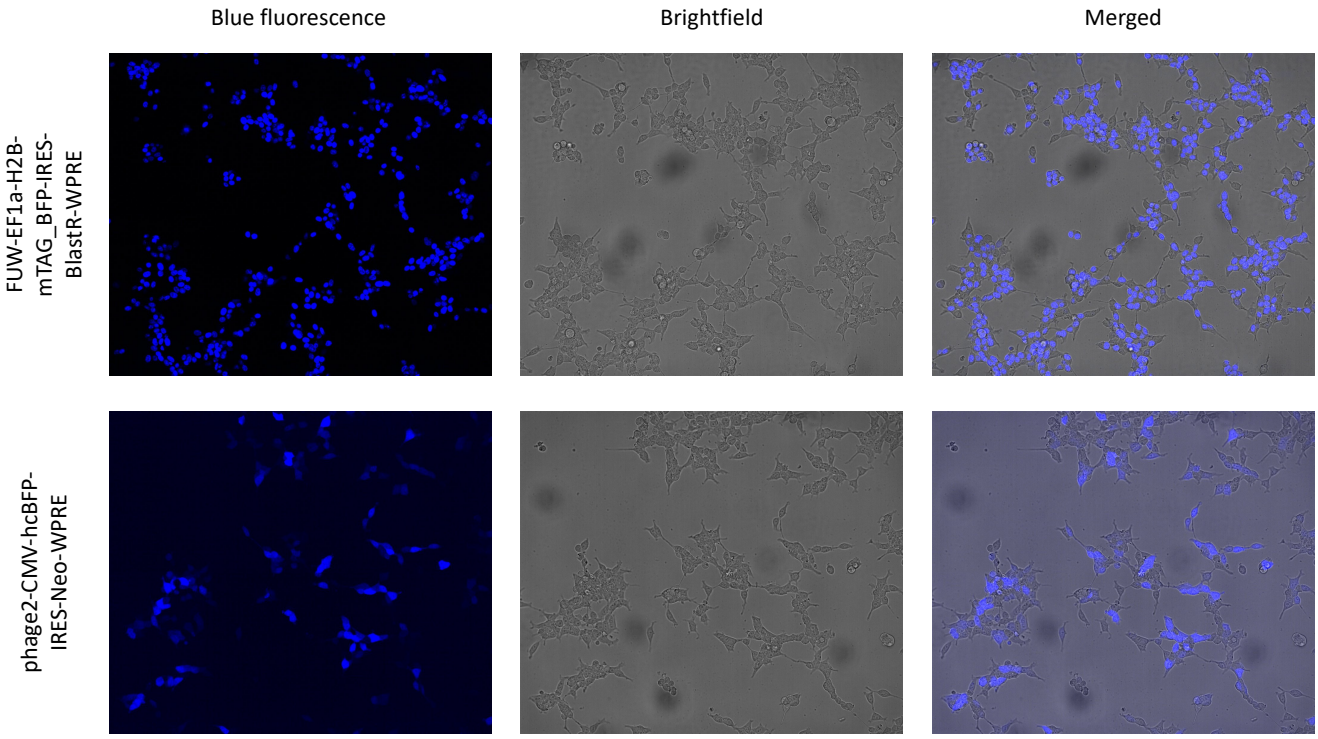

Figure 18: Overview of different BFP plasmids used. HEK293T cells transfected with respective BFP plasmid. 10x magnification.

Discussion and conclusion

In order to measure EV-mediated RNA transfer in a more in vivo-like representation an optimization of spheroid formation was performed. Both HEK293T and MCF-7 cells formed round and dense structures in ultra-low adherence plates, whereas MDA-MB-231 did not. 3D-imaging and 3D reconstruction showed that these structures are cup-shaped hollow structures which most likely prevents the formation of a necrotic core, one of the key characteristics of a tumor spheroid. Whilst this could be caused by limitations due to the 3D imaging by the microscope or by the 3D reconstruction software, looking with the naked eye at these structures in a suspension of PBS confirmed that they have a somewhat flat composition instead of a spherical one. 3D-imaging of spheroids by Li et al., also shows cup-shaped spheroids using a different microscope and software, indicating that this is not an uncommon problem (31). The lack of a necrotic core is supported by Sant et al., who performed ethidium homodimer dead cell staining on spheroids grown in ultra-low adherence plates. These spheroids are comparable in shape and size to the spheroids shown in this paper and showed only small spots of necrosis under normal conditions, but no necrotic core was formed (32). It is also suggested that because of the hollowness of the spheroids EV-mediated RNA transfer will take place over longer distances since EVs in a compact spheroid are more likely to be taken up by cells in close proximity to the cell which released the EV.

Optimization with larger cell counts or culturing in tumorsphere medium did not improve spheroid formation. Adding Geltrex or Matrigel did seem to improve spheroid formation somewhat, but the structures remained relatively bowl-shaped. For future experiments spheroid formation could be improved by encapsulating such a structure in a droplet of Geltrex or Matrigel.
It was found that these spheroid-like structures can be disrupted to single cells and analyzed by measuring mCherry- and eGFP signal by flow cytometry, proving its usefulness for future experiments measuring EV-mediated RNA transfer in a 3D environment.
Overall, the protocols used for spheroid formation in ultra-low attachment plates need further optimization to better mimic *in vivo* tumors.

Newly made MCF-7 targeting- and non-targeting sgRNA donor lines behaved as expected in combination with HEK293T stoplight reporter cells. However, unexpectedly a combination of MCF-7 targeting sgRNA donor cells and MCF-7 stoplight reporter cells did not result in a measurable sgRNA transfer. Further testing showed that also HEK293T donor cells cannot successfully transfer sgRNA to HEK293T stoplight cells, proving that this is not limited to MCF-7. An MDA-MB-231 donor/reporter combination has been reported to show EV-mediated RNA transfer, proving that this is cell type specific (figure 19) (9). Since all these cell types are proven to be functional donor-, and reporter lines these results were unexpected. The inability for EV-mediated RNA transfer between donor and reporter cells of the same cell type might be caused by a missing receptor ligand interaction, preventing the uptake of sgRNA-containing EVs. Comparable results have not been published and it would be interesting to investigate this further. A better understanding of this mechanism could lead to a possible drug target for inhibiting intratumoral RNA transfer by EVs, possibly lowering the chances of metastasis. A first step would be to identify the difference in receptors on EVs produced by MCF-7 with those on e.g., MDA-MB-231. This information might teach us more about this cell type specificity and the uptake mechanisms involved. T47D donor cells were not successful for EV-mediated RNA transfer, which suggests low loading of sgRNA into EVs. This could be confirmed by isolating EVs produced by T47D and add a set number to a reporter cell line. This can be compared by adding the same number of EVs isolated from another donor line of which we know can successfully transport sgRNA via EVs. Any difference in eGFP expression is most likely caused by sgRNA loading.

In order to discern sgRNA expressing donor cells from mCherry positive reporter cells lentiviral transduction of donor cells was performed to stably express BFP. Flow cytometry measurements showed an BFP expression between 40- and 70%. Whilst these percentages are high enough for fluorescence microscopy cell sorting could be used to increase these values which might be necessary for flow cytometry protocols. The cloned construct using a nucleus staining BFP can be used in future experiments for both fluorescence microscopy as well as flow cytometry.

EV-mediated transport of RNAs is a promising field in cancer research. There is still a long way to go but with these new insights we might be a step closer to finding new therapies to combat growing incidences of cancer.

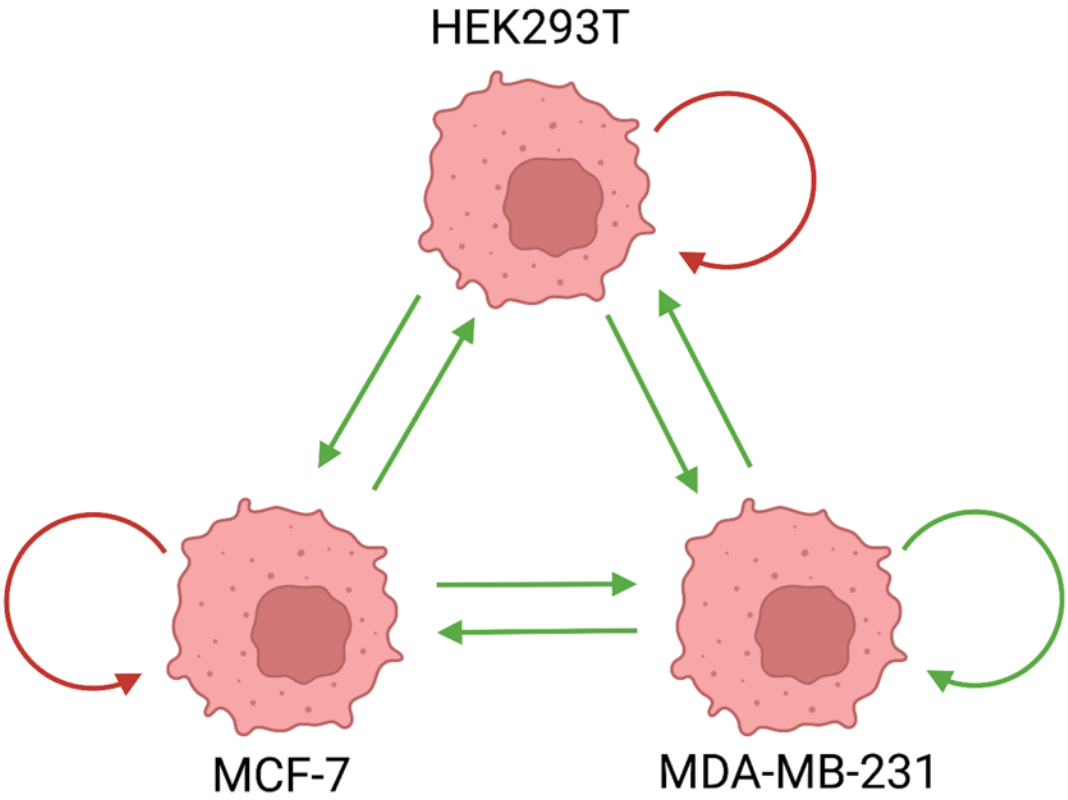

Figure 19: Overview of cell types which showed EV-mediated sgRNA transfer between each other in a donor: reporter relation. (some conditions N=2).

Acknowledgements

Special thanks to dr. Olivier de Jong for his supervision and for giving me the opportunity to work on this project. Thanks to dr. Pieter Vader for being my second examiner. For her help around the lab and setting up the protocol for 3D reconstruction of spheroids I would like to thank Vivian Hegeman. Thanks to Esmeralda Bosman for setting up 3D imaging protocols and for letting me use her BFP mTAG plasmid.

References

1. Worldwide cancer incidence statistics | Cancer Research UK [Internet]. [cited 2023 Aug 8]. Available from: https://www.cancerresearchuk.org/health-professional/cancer-statistics/worldwide-cancer/incidence
2. Xiao Y, Yu D. Tumor microenvironment as a therapeutic target in cancer. Pharmacol Ther. 2021;
3. Maacha S, Bhat AA, Jimenez L, Raza A, Haris M, Uddin S, et al. Extracellular vesicles-mediated intercellular communication: Roles in the tumor microenvironment and anti-cancer drug resistance. Mol Cancer. 2019;18(1).
4. Hinshaw DC, Shevde LA. The Tumor Microenvironment Innately Modulates Cancer Progression. Cancer Res [Internet]. 2019 Sep 9 [cited 2023 Sep 12];79(18):4557. Available from: /pmc/articles/PMC6744958/
5. Clancy JW, D'Souza-Schorey C. Tumor-Derived Extracellular Vesicles: Multifunctional Entities in the Tumor Microenvironment. Annu Rev Pathol [Internet]. 2023 Jan 1 [cited 2023 Sep 15];18:205. Available from: /pmc/articles/PMC10410237/
6. Fernández JP, Luddy KA, Harmon C, O'Farrelly C. Hepatic Tumor Microenvironments and Effects on NK Cell Phenotype and Function. Int J Mol Sci [Internet]. 2019 Sep 1 [cited 2023 Sep 16];20(17). Available from: /pmc/articles/PMC6747260/
7. Abels ER, Breakfield XO. Introduction to Extracellular Vesicles: Biogenesis, RNA Cargo Selection, Content, Release, and Uptake. Cell Mol Neurobiol. 36(3): 301.
8. Zomer A, Maynard C, Verweij FJ, Kamermans A, Schäfer R, Beerling E, et al. In vivo imaging reveals extracellular vesicle-mediated phenocopying of metastatic behavior. Cell. 2015;161(5):1046–57.
9. de Jong OG, Murphy DE, Mäger I, Willms E, Garcia-Guerra A, Gitz-Francois JJ, et al. A CRISPR-Cas9-based reporter system for single-cell detection of extracellular vesicle-mediated functional transfer of RNA. Nat Commun [Internet]. 2020 Dec 1 [cited 2023 Sep 23];11(1). Available from: /pmc/articles/PMC7048928/
10. Ma Y, Zhang L, Huang X. Genome modification by CRISPR/Cas9. FEBS J [Internet]. 2014 Dec 1 [cited 2023 Sep 18];281(23):5186–93. Available from: https://onlinelibrary.wiley.com/doi/full/10.1111/febs.13110
11. Xue C, Greene EC. DNA repair pathway choices in CRISPR-Cas9 mediated genome editing. Trends Genet. 2021;37(7):639–56.
12. Ishiguro T, Ohata H, Sato A, Yamawaki K, Enomoto T, Okamoto K. Tumor-derived spheroids: Relevance to cancer stem cells and clinical applications. Cancer Sci. 2017;108(3):283–9.
13. Habanjar O, Diab-Assaf M, Caldefie-Chezet F, Delort L. 3D cell culture systems: Tumor application, advantages, and disadvantages. Int J Mol Sci. 2021;22(22).
14. Lotsberg ML, Røsland G V, Rayford AJ, Dyrstad SE, Ekanger CT, Lu N, et al. Intrinsic Differences in Spatiotemporal Organization and Stromal Cell Interactions Between Isogenic Lung Cancer Cells of Epithelial and Mesenchymal Phenotypes Revealed by

High-Dimensional Single-Cell Analysis of Heterotypic 3D Spheroid Models. [cited 2023 Aug 8]; Available from: www.frontiersin.org
15. Ryu NE, Lee SH, Park H. Spheroid culture system methods and applications for mesenchymal stem cells. Cells. 2019;8(12):1–13.
16. Froehlich K, Haeger JD, Heger J, Pastuschek J, Photini SM, Yan Y, et al. Generation of Multicellular Breast Cancer Tumor Spheroids: Comparison of Different Protocols. J Mammary Gland Biol Neoplasia. 2016;21(3–4):89–98.
17. Tung YC, Hsiao AY, Allen SG, Torisawa YS, Ho M, Takayama S. High-throughput 3D spheroid culture and drug testing using a 384 hanging drop array †.
18. Costa EC, de Melo-Diogo D, Moreira AF, Carvalho MP, Correia IJ. Spheroids Formation on Non-Adhesive Surfaces by Liquid Overlay Technique: Considerations and Practical Approaches. Biotechnol J [Internet]. 2018 Jan 1 [cited 2023 Sep 21];13(1):1700417. Available from: https://onlinelibrary-wiley-com.proxy.library.uu.nl/doi/full/10.1002/biot.201700417
19. Li Y, Kumacheva E. Hydrogel microenvironments for cancer spheroid growth and drug screening. Sci Adv [Internet]. 2018 Apr 27 [cited 2023 Sep 21];4(4). Available from: /pmc/articles/PMC5922799/
20. 293T - CRL-3216 | ATCC [Internet]. [cited 2023 Aug 7]. Available from: https://www.atcc.org/products/crl-3216
21. MDA-MB-231 - CRM-HTB-26 | ATCC [Internet]. [cited 2023 Aug 7]. Available from: https://www.atcc.org/products/crm-htb-26
22. Welsh J. Animal Models for Studying Prevention and Treatment of Breast Cancer.
23. 3D Tumorsphere Medium XF - PromoCell [Internet]. [cited 2023 Aug 7]. Available from: https://promocell.com/product/3d-tumorsphere-medium-xf/#tab-reference_literature
24. Wang C, Shi M, Ji J, Cai Q, Jiang J, Zhang H, et al. A self-enforcing HOXA11/Stat3 feedback loop promotes stemness properties and peritoneal metastasis in gastric cancer cells. Issue 25 Theranostics [Internet]. 2019 [cited 2023 Aug 7];9(25):7628–47. Available from: http://www.thno.org://creativecommons.org/licenses/by/4.0/
25. Costa EC, de Melo-Diogo D, Moreira AF, Carvalho MP, Correia IJ. Spheroids Formation on Non-Adhesive Surfaces by Liquid Overlay Technique: Considerations and Practical Approaches. Biotechnol J. 2018 Jan 1;13(1).
26. Benton G, Arnaoutova I, George J, Kleinman HK, Koblinski J. Matrigel: From discovery and ECM mimicry to assays and models for cancer research. Adv Drug Deliv Rev. 2014;79:3–18.
27. T-47D - HTB-133 | ATCC [Internet]. [cited 2023 Aug 9]. Available from: https://www.atcc.org/products/htb-133#detailed-product-information
28. Rizwan A, Cheng M, Bhujwalla ZM, Krishnamachary B, Jiang L, Glunde K. Breast cancer cell adhesome and degradome interact to drive metastasis. npj Breast Cancer 2015 1:1 [Internet]. 2015 Oct 28 [cited 2023 Aug 9];1(1):1–11. Available from: https://www.nature.com/articles/npjbcancer201517
29. Park CH, Kimler BF, Smith TK. Comparison of the supravital DNA dyes Hoechst 33342 and DAPI for flow cytometry and clonogenicity studies of human leukemic marrow cells. Exp Hematol. 1985 Nov 13;13(10):1039–43.
30. Subach OM, Cranfill PJ, Davidson MW, Verkhusha V V. An Enhanced Monomeric Blue Fluorescent Protein with the High Chemical Stability of the Chromophore. PLoS One

[Internet]. 2011 Dec 8 [cited 2023 Aug 10];6(12):28674. Available from: /pmc/articles/PMC3234270/

31. Li L, Zhou Q, Voss TC, Quick KL, LaBarbera D V. High-throughput Imaging: Focusing In On Drug Discovery in 3D. Methods [Internet]. 2016 Mar 3 [cited 2023 Aug 11];96:97. Available from: /pmc/articles/PMC4766031/

32. Sant S, Johnston PA. The Production of 3D Tumor Spheroids for Cancer Drug Discovery. Drug Discov Today Technol [Internet]. 2017 Mar 1 [cited 2023 Aug 11];23:27. Available from: /pmc/articles/PMC5497458/

Supplementary figures

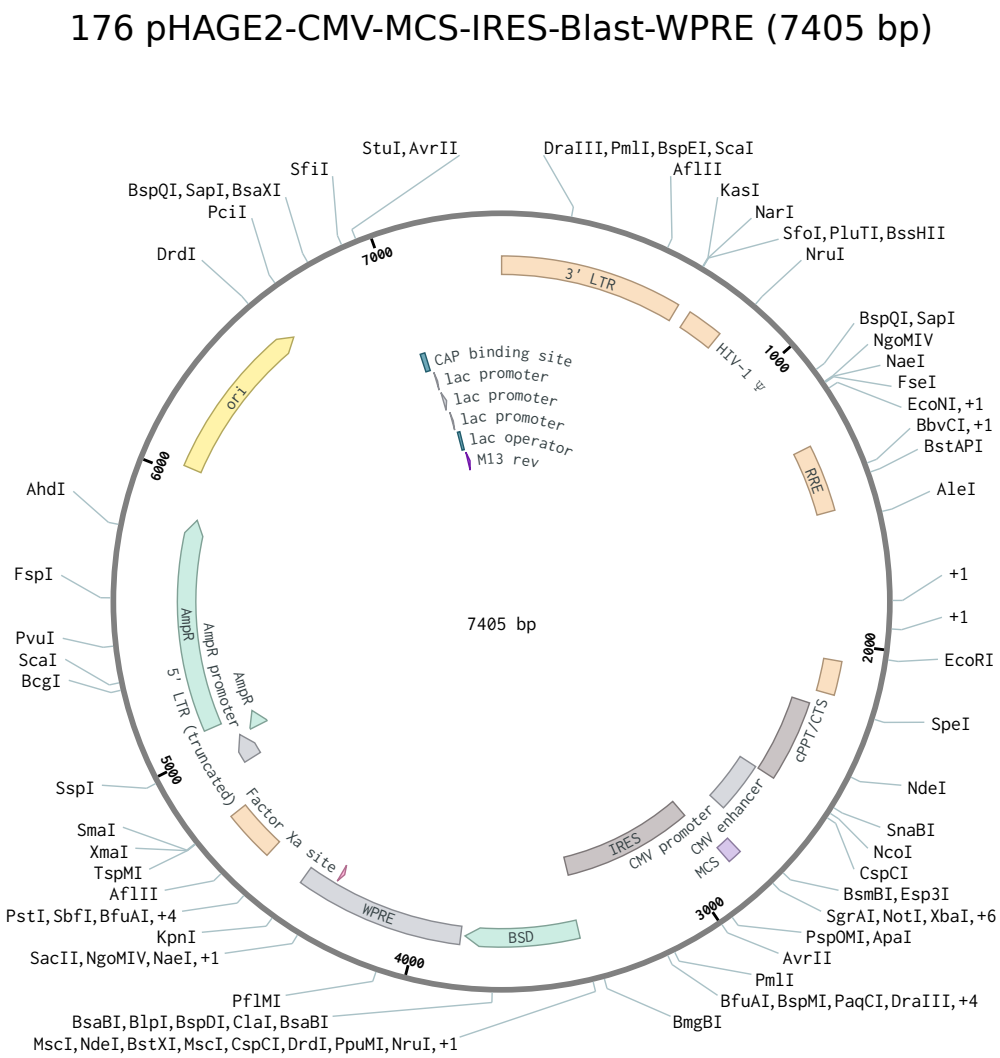

Supplementary figure 1: Genomic map of pHAGE2-CMV-MCS-IRES-Blast-WPRE.

266 FUW-EF1a-H2B-mTAG_BFP-IRES-PuroR-WPRE (1096...

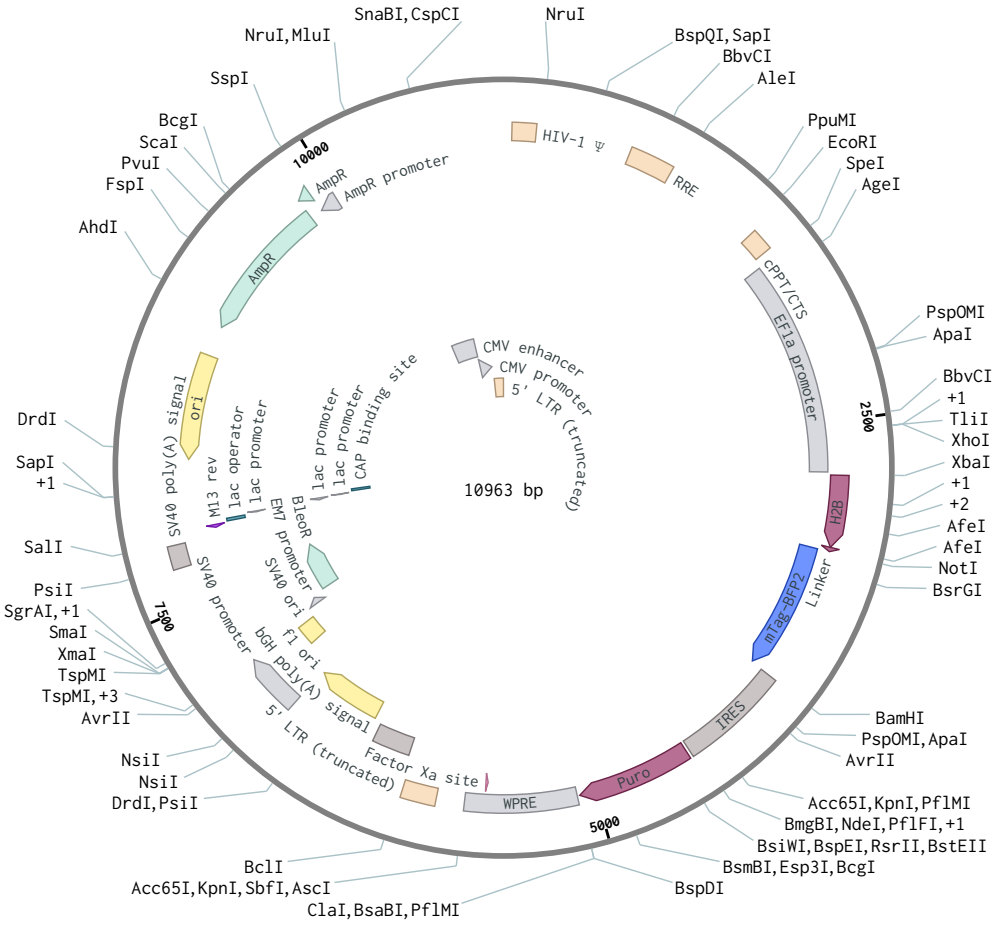

Supplementary figure 2: Genomic map of FUW-EF1a-H2B-mTAG_BFP-IRES-PuroR-WPRE.

328 FUW-EF1a-H2B-mTAG_BFP-IRES-BlastR-WPRE (107...

Supplementary figure 3: Genomic map of FUW-EF1a-H2B-mTAG_BFP-IRES-BlastR-WPRE.

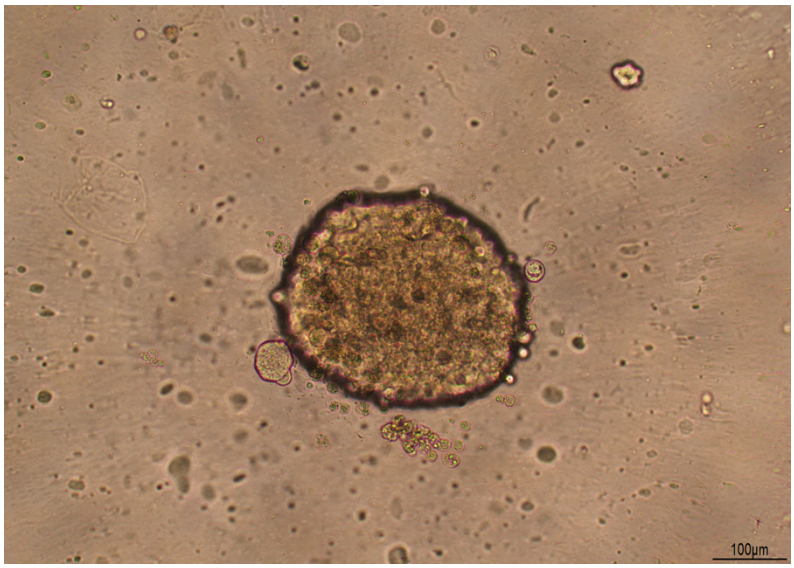

Supplementary figure 4: Spheroid formation of T47D. 10.000 cells seeded at d0, cultured for 5 days in DMEM F12 + 10% FBS. Scalebar = 100 µm.